Frontiers in Bioscience Landmark

Front. Biosci. (Landmark Ed) **2024**; 29(2): 69
https://doi.org/10.31083/j.fbl2902069

Original Research

SPC25 Functions as a Prognostic-Related Biomarker, and Its High Expression Correlates with Tumor Immune Infiltration and UCEC Progression

Li-xin Liao[1], Meng Zhang[1], Xin Xu[1], Shan Zhang[1], Yu-zhen Guo[1,*]

[1]Department of Gynecology, The Second Hospital & Clinical Medical School, Lanzhou University, 730030 Lanzhou, Gansu, China
*Correspondence: guoyz@lzu.edu.cn (Yu-zhen Guo)
Academic Editor: Yudong Cai
Submitted: 19 September 2023 Revised: 28 December 2023 Accepted: 2 January 2024 Published: 20 February 2024

Abstract

Background: Most tumor tissues expressed spindle pole body component 25 (*SPC25*), one of the four subunits of the NDC80 complex, at greater levels compared to surrounding normal tissues. According to earlier researches, this subunit strongly encouraged tumor cell proliferation and tumor growth, which resulted in worse prognoses in patients with hepatocellular, breast, lung, and prostate cancer. Precisely because *SPC25*'s role in uterine corpus endometrial carcinoma (UCEC) is understudied, we chose to concentrate on UCEC for gaining a more scientific and thorough understanding of *SPC25*. **Methods**: Along with examining *SPC25*'s differential expression, prognostic significance, and biological function in UCEC, our research sought to clarify the underlying mechanism by which *SPC25* influences the course of UCEC and patient prognosis from the viewpoints of methylation and immune infiltration. **Results**: We observed differential expression of *SPC25* gene in different clinicopathological features of UCEC and identified *SPC25* as a hazard factor for poorer overall survival (OS), disease-specific survival (DSS), and progress free interval (PFI) in UCEC, particularly in its multiple clinical subtypes. In addition, we also discovered that *SPC25* and its co-expressed genes mostly engaged in biological processes and signal transduction routes linked to cell cycle and cell division in UCEC. After investigating *SPC25*'s methylation status, we discovered that patients with UCEC had elevated *SPC25* expression and a poor prognosis due to hypomethylation of CpG sites in the *SPC25* gene sequence. Finally, we investigated *SPC25*'s potential role in immunotherapy and discovered that *SPC25* might alter the major immune cell infiltration levels in the tumor microenvironment (TME) by regulating the expression of immunoregulatory molecules and chemokines, which would be beneficial for *SPC25* to control the progression of UCEC. **Conclusions**: In conclusion, *SPC25* was a useful predictive biomarker as well as a possible therapeutic target for UCEC.

Keywords: SPC25; UCEC; prognosis; coexpression; methylation; immune

1. Introduction

Mitosis maintains the genetic properties of any multicellular organism throughout entire life cycle. Every time the mother cell divides, the chromosomes are evenly distributed among the daughter cells due to the action of the mitotic spindle [1]. The NDC80 complex which is an extremely conserved kinetochore protein from yeast to humans, is an approximately 57 nm elongated heterotetramer consisting of NDC80 (NDC80P, HEC1, nuclear division cycle 80), NUF2 (NUF2P, NUF2 component of NDC80 kinetochore complex), SPC24 (SPC24P, spindle pole body component 24), and SPC25 (SPC25P, spindle pole body component 25). At its SPC24/SPC25 globular end, the complex connects the centromere-proximal inner kinetochore layer to the microtubule-binding outer kinetochore layer at its NDC80/NUF2 globular end [2,3]. It is crucial that spindle microtubules attach to the chromosome kinetochores through the NDC80 complex during cell division [4]. *NDC80* has been considered as a major player in cancers' initiation, development, and spread in the last few years. *NDC80* was abundantly expressed in various cancers and promoted tumor growth through the reduction of apoptosis and increasing cell cycle efficiency, resulting in poor survival and prognosis of cancer patients [5–9]. *SPC25* overexpression has been found in recent researches to enhance tumor growth and metastasis in hepatocellular carcinoma (HCC), as well as a worse prognosis for HCC patients [10–13]. The same conclusion appears in the study of lung cancer [14–16], prostate cancer (PCa) [17,18], breast cancer (BC) [19], and neurodegeneration [20]. *SPC25* is also necessary for chromosomal alignment, spindle formation, and effective spindle checkpoint signaling during meiosis, according to research [21].

The number of deaths linked to endometrial cancer (EC) is rising, with an estimated 1–2% yearly increase in the disease's incidence. But no fresh medications were authorized for the treatment of EC. There are currently only two Food and Drug Administration (FDA)-approved medications for the treatment of EC, despite the fact that numerous medications are approved for the treatment of ovarian, fallopian tube, and primary peritoneal cancers. This highlights the need for novel therapies to treat advanced, recurrent, and metastatic EC [22].

Our research goal was to determine *SPC25*'s differential expression, prognostic value, biological functions, and its potential in immune infiltration in uterine corpus endometrial carcinoma (UCEC) by providing a more systematic and comprehensive perspective. Thus, we looked into the associations between *SPC25*'s expression and various clinicopathological features, clinical outcomes in various clinical subgroups, and coexpression network analyses in UCEC. Moreover, we focused on the methylation level of *SPC25* in UCEC and its corresponding predictive significance, and explored the potential mechanism of *SPC25* expression and methylation status in UCEC progression.

In our results, *SPC25* was shown to be significantly associated with clinical stage, histologic grade, histological type, radiation therapy, tumor invasion, weight, primary therapy outcome, molecular subtype, immune subtype, and TP53 muation status. Additionally, elevated *SPC25* expression might result in poorer overall survival (OS), disease-specific survival (DSS), and progress free interval (PFI), especially in distinct clinical subgroups of UCEC. Furthermore, we also obtained the *SPC25* co-expressed genes, which included 1981 positively correlated genes and 2213 negatively correlated genes. These genes primarily took part in chromosome segregation, DNA replication, cell cycle checkpoint, spindle organization, and negative regulation of cell cycle process. Co-expressed genes were enriched in Cell cycle, Spliceosome, DNA replication, RNA transport, and Oocyte meiosis. Most importantly, the majority of the *CpG* sites in the *SPC25* DNA sequence were hypomethylated, which decreased patient survival and had a negative correlation with immunosuppressive state in the tumor microenvironment (TME). Therefore, it was hypothesized that hypomethylation of the *SPC25* promoter caused the overexpression of *SPC25* mRNA and protein, and this in turn decreased the expression of chemokines and their receptors, which reduced the aggregation of major immune cells to the tumor site and exerted antitumor immunity, ultimately worsening the disease and shortening the patient's survival time.

Based on these findings, we concluded that *SPC25* would modify the composition and immunological processes of TME, which in turn might alter antitumor immunity and impact the course and outcomes of disease. So we speculated that *SPC25* might be a significant prognostic biomarker and that *SPC25* might work as a potential molecular biomarker to predict immunotherapy response or a novel anticancer immunotherapy target to achieve promising treatment outcomes in UCEC.

2. Materials and Methods

2.1 SPC25 mRNA and Protein Expression Differences between Endometrial Cancer and Normal Tissues

In our study, we investigated the levels of *SPC25* mRNA expression in tissue samples of endometrial cancer and endometrial hyperplasia using a UCEC dataset (GSE106191) that was retrieved from the gene expression omnibus (GEO) database (https://www.ncbi.nlm.nih.gov/geo/). The ggplot2 package [3.3.6] was utilized for data visualization, while the stats package [4.2.1] and car package [3.1-0] were employed for statistical analysis. The protein levels of SPC25 in UCEC were then determined using the university of alabama at birmingham cancer data analysis portal (UALCAN) database (http://ualcan.path.uab.edu/) [23–25], an internet application that allows users to analyze the cancer genome atlas (TCGA) and gene transcription data online. We also explored the SPC25 protein expression in endometrial cancer tissues via the Human Protein Atlas (HPA) (https://proteinatlas.org/) [26,27] which contains the human gene expression profile information for both normal and malignant tissues protein levels. Statistics were considered significant when $p < 0.05$.

We gathered tumor tissues and their paired adjacent normal tissues from 12 patients with endometrial carcinoma who received surgical treatment at the Department of Gynecology of the Second Hospital of Lanzhou University from March 2023 to June 2023. Prior to surgery, no additional therapies were administered to any of the 12 patients. This study was conducted in line with the tenets of the Helsinki Declaration and was approved by the Ethics Committee at the Second Hospital of Lanzhou University. Each patient voluntarily gave their informed permission. SPC25 protein expression was detected by Western blotting assay. In brief, lysing both normal and tumor tissues in RIPA (R0010, Solarbio, Beijing, China) lysis solution containing PMSF (P0100, Solarbio, Beijing, China) for 30 minutes allowed for the extraction of all tissue proteins. Following the protein solution's separation using 10% SDS-PAGE (P1200, Solarbio), the resultant product was subsequently transferred to PVDF membranes. After blocking the PVDF (YA1700, Solarbio) membranes for 30 minutes at room temperature with a blocking solution (P0252, Beyotime, Shanghai, China), they were incubated with primary antibodies for the whole overnight duration at 4 °C. Next day, secondary antibodies were incubated on the membranes for 2 hours at room temperature. Immunoreactive signals were recognized utilizing enhanced chemiluminescence (ECL, PE0010, Solarbio). The primary antibodies utilized were mouse anti-human SPC25 monoclonal antibody (26 kDa; 1:500; TA806559S, OriGene, Jiangsu, China) and mouse anti-human GAPDH monoclonal antibody (35.9 kDa; 1:2000; TA802519S, OriGene).

2.2 Relationships between SPC25 Expression and a Variety of Clinical Traits in UCEC

Firstly, we utilized the "Clinical" and "Subtype" modules of TISIDB (an integrated repository portal for tumor-immune system interactions) website (http://cis.hku.hk/TISIDB/) [28] to observe the correlations between *SPC25* expression level and cancer stages, tumor grades, molecular subtypes, and immune subtypes of UCEC. Then, the Xi-

antao Academic website (https://www.xiantao.love/) [29] provided box plots for *SPC25* expression levels of individuals with various clinical features in UCEC. The RNA-seq data and linked clinical data were retrieved from the TCGA database (https://portal.gdc.cancer.gov/) in level 3 HTSeq-fragments per kilobase per million (FPKM) format, translated to transcripts per million reads (TPM) format, and analyzed after log2 conversion. For statistical analysis and data visualization, the ggplot2 package [3.3.6] was utilized, along with the stats package [4.2.1] and car package [3.1-0]. To detect two groups of data, the Shapiro-Wilk normality test, Kruskal-Wallis test, and Multiple hypothesis test (Dunn's test) with Bonferroni's method to adjust significant level were employed. Ultimatly, in order to verify and strengthen the previous findings, we uesd the UALCAN database to analyze the connection between *SPC25* gene expression and clinicopathological characteristics in UCEC. A statistically significant *p*-value was defined as one less than 0.05.

2.3 Survival Prognosis Analysis in Different UCEC Clinical Subgroups

First, we evaluated the diagnostic ability of *SPC25* for UCEC utilizing the receiver operating characteristic curve (ROC curve) of the Xiantao Academic web. Utilizing the pROC program [1.18.0], the data underwent ROC analysis, and ggplot2 [3.3.6] was utilized to display the outcomes. Next, we investigated how *SPC25* affected the OS, relapse free survival (RFS), DSS, and PFI of UCEC using online tools like Kaplan-Meier Plotter (http://kmplot.com/analysis/) [30] and Xiantao Academic. We further looked into the relationships between *SPC25* expression and prognosis (OS, DSS, and PFI) in distinct UCEC clinical subgroups using Kaplan-Meier plots on the Xiantao Academic website [31]. In this website, the median *SPC25* expression was used as a cutoff value to classify groups (low expression group: 0–50%; high expression group: 50–100%). For the proportional hazards assumption test and fitting survival regression, the Survival package [3.3.1] was utilized. The ggplot2 and survminer programs [3.3.6] provided visual representations of the findings. In the hypothesis test, the log-rank test and cox regression were adopted. *p* value less than 0.05 means statistical significance.

2.4 SPC25 Coexpression Network Analyse in UCEC

we used two of three analytical modules in the LinkedOmics database (http://linkedomics.org/login.php) [32]: LinkFinder and LinkInterpreter. We utilized LinkFinder to find the *SPC25* coexpressed genes using the Pearson correlation test, and the findings were shown using a volcano plot, heat maps, and scatter diagrams. Subsequently, utilizing gene set enrichment analysis (GSEA), we applied LinkInterpreter to the GO_BP (gene ontology biological process) and KEGG (kyoto encyclopedia of genes and genomes) pathways of *SPC25* and its coexpressed genes. As statistically significant, a *p*-value of less than 0.05 was considered.

Then, we opened the web page (https://cn.string-db.org/) of STRING (search tool for the retrieval of interacting genes/proteins) [33] to get SPC25 binding proteins that have been experimentally verified and we calculated the intersection of the two sets of data—SPC25 binding proteins and *SPC25*-coexpressed genes—using Draw Venn Diagram (https://bioinformatics.psb.ugent.be/webtools/Venn/). To make the results more convincing, we used the function of "Single gene coexpression heat map" in Xiantao Academic to verify the correlation between *SPC25* and the genes in the cell cycle pathway network obtained from PathCards website (https://pathcards.genecards.org/) [34]. Coexpression heat maps were produced using the ggplot2 package [3.3.6] to illustrate the analysis findings (ns, $p \geq 0.05$; *, $p < 0.05$; **, $p < 0.01$; ***, $p < 0.001$).

2.5 DNA Methylation Status in the CpG Islands of the SPC25 Gene and Their Prognostic Value in UCEC

DNA hypermethylation at promoters can result in gene silence [35]. To further pinpoint the mechanisms underlying the upregulation of *SPC25* in UCEC, the methylation levels of *SPC25* in the UCEC dataset were analyzed via the UALCAN database. In addition, we also compared the differential expression of *SPC25* and its promoter methylation status in UCEC patients with various tumor grades (grades 1, 2, 3, and 4). Not only does DNA methylation during carcinogenesis affect gene expression, but also the prognosis of cancer patients [36]. MethSurv (https://biit.cs.ut.ee/methsurv/) [37] is a website that uses TCGA data to perform survival analysis based on DNA methylation biomarkers. DNA methylation status of the *SPC25* gene's CpG sites and the prognostic significance of these CpG sites in UCEC were explored in the UCEC–TCGA dataset using the MethSurv database. *p* value less than 0.05 means statistical significance.

2.6 Associations of SPC25 Expression and Its Methylation Status with Immune Cells, Immunomodulators, and Chemokines in UCEC

The TISIDB database (http://cis.hku.hk/TISIDB) [28] is a web server for the interaction analysis of the immune system and tumor that can help forecast the effectiveness of immunotherapy. In our work, the associations between *SPC25* expression and its methylation status and immune cells, immunomodulators, and chemokines were evaluated by the Xiantao Academic and TISIDB websites. The ggplot2 package [3.3.6] was used to illustrate the analysis findings, which was carried out with R programming language [4.2.1].

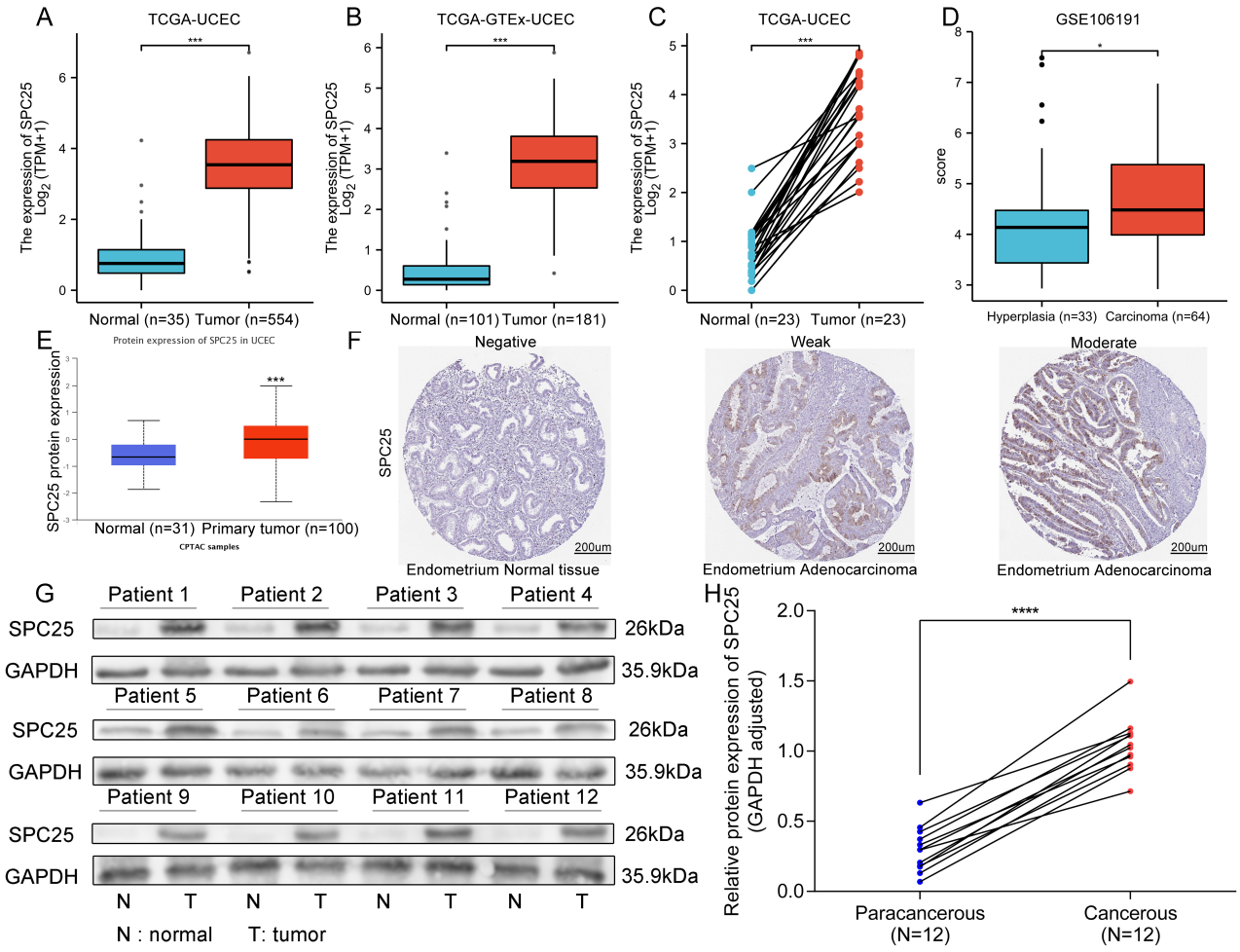

Fig. 1. Spindle pole body component 25 (*SPC25*) mRNA and protein expression in uterine corpus endometrial carcinoma (UCEC). (A–C) *SPC25* mRNA expression levels in endometrial cancer patients and matched adjacent normal samples. (D) *SPC25* mRNA expression levels were upregulated in the endometrial cancer tissues compared to endometrial hyperplasia tissues in the GSE106191 dataset. (E,F) SPC25 protein expression levels based on the university of alabama at birmingham cancer data analysis portal (UALCAN) and Human Protein Atlas. (G,H) Utilizing Western blotting, the levels of SPC25 protein expression were confirmed. *$p < 0.05$; ***, $p < 0.001$; ****, $p < 0.0001$.

2.7 Statistical Analysis

Examining the *SPC25* expression differences between normal (or hyperplasia) and malignant tissues was done Utilizing the Wilcoxon rank sum test (Mann-Whitney U test), Paired Samples *T* test, and Independent Sample *T* test. The Kruskal-Wallis test, Dunn's test, Wilcoxon rank sum test, Welch one-way ANOVA test, Games-Howell test, and Independent-Sample *T* Test were utilized to explore the association between *SPC25* expression and clinicopathological features. The area under the curve (AUC) acquired from the time-dependent ROC curve analysis was employed to assess the *SPC25*'s UCEC diagnosis accuracy. Additionally, utilizing the Kaplan-Meier (KM) curve, which employs the Log-rank test and Cox regression, the potential predictive significance of *SPC25* expression in UCEC patients with different clinical pathological features was evaluated. Pearson Correlation Analysis was utilized to search for gene sets that correlated positively and negatively with *SPC25* expression in UCEC and conduct gene set enrichment analysis (GSEA) analysis. The expression association between *SPC25* and genes relevant to the cell cycle pathway network as well as immunological checkpoints in UCEC was examined using Spearman association Analysis. The influence of each *SPC25* gene DNA methylation site's methylation status on the UCEC patients' prognosis was examined using the likelihood ratio test. To investigate the relationship between *SPC25* expression and the enrichment of 24 different types of immune cells in UCEC TME, Spearman Correlation Analysis was employed. To compare the immune cell enrichment scores of the high and low *SPC25* expression groups, the Wilcoxon rank sum test was employed. At $p < 0.05$, statistical significance was established.

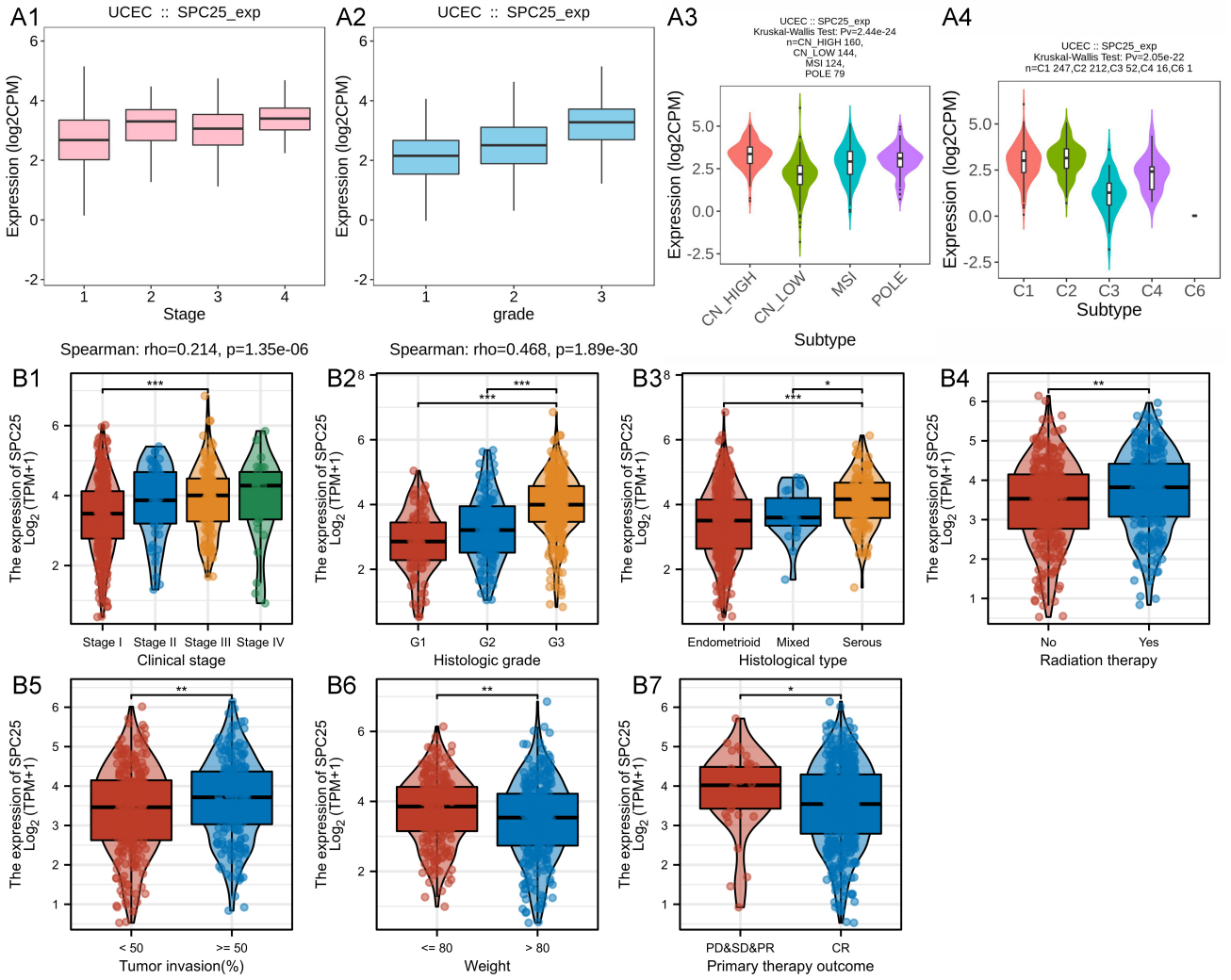

Fig. 2. Relationships between *SPC25* expression and several clinical features in UCEC analyzed by the TISIDB (A1–A4) and Xiantao Academic (B1–B7) databases. (A1) Cancer stage; (A2) Tumor grade; (A3) Molecular subtype; (A4) Immune subtype; (B1) Clinical stage; (B2) Histologic grade; (B3) Histological type; (B4) Radiation therapy; (B5) Tumor invasion (%); (B6) Weight; (B7) Primary therapy outcome. *$p < 0.05$; **$p < 0.01$; ***$p < 0.001$. PD, progressive disease; SD, stable disease; PR, partial response; CR, complete response.

3. Results

3.1 SPC25 was Upregulated in UCEC

We discovered that *SPC25* was highly expressed in UCEC (Fig. 1A,B). We also verified that *SPC25*'s expression was considerably higher in UCEC than in matched nearby normal tissues (Fig. 1C). Additionally, the GSE106191 dataset's endometrial cancer tissues showed greater levels of *SPC25* expression than the endometrial hyperplasia tissues ($p < 0.05$) (Fig. 1D). Results from the UALCAN database and immunohistochemistry (IHC) staining further indicated that SPC25's protein expression was increased in endometrial cancer tissues (Fig. 1E,F). The outcomes of Western blotting on 12 matched pairs of tumor and surrounding tissues confirmed once more that endometrial cancer had much greater levels of SPC25 protein than healthy tissues (Fig. 1G,H).

3.2 SPC25 was Linked to a Variety of Clinical Features in UCEC

The results of TISIDB indicated that the expression level of *SPC25* was closely related to the cancer stages ($p = 1.35 \times 10^{-6}$), tumor grades ($p = 1.89 \times 10^{-30}$), molecular subtypes ($p = 2.44 \times 10^{-24}$), and immune subtypes ($p = 2.05 \times 10^{-22}$) of UCEC (Fig. 2A1–A4, respectively). We also used Xiantao Academic to present the relationships between *SPC25* and various clinical features in UCEC, and discovered that *SPC25* was expressed at a greater level in patients with stage III, histologic grade 3, histological type of serous, radiation therapy (yes), and tumor invasion (%) (≥50) while it was expressed at a lower level in patients with weight >80 and primary therapy outcome (CR) (Fig. 2B1–B7, respectively). Then, using the UALCAN database, we looked at *SPC25* expression in UCEC

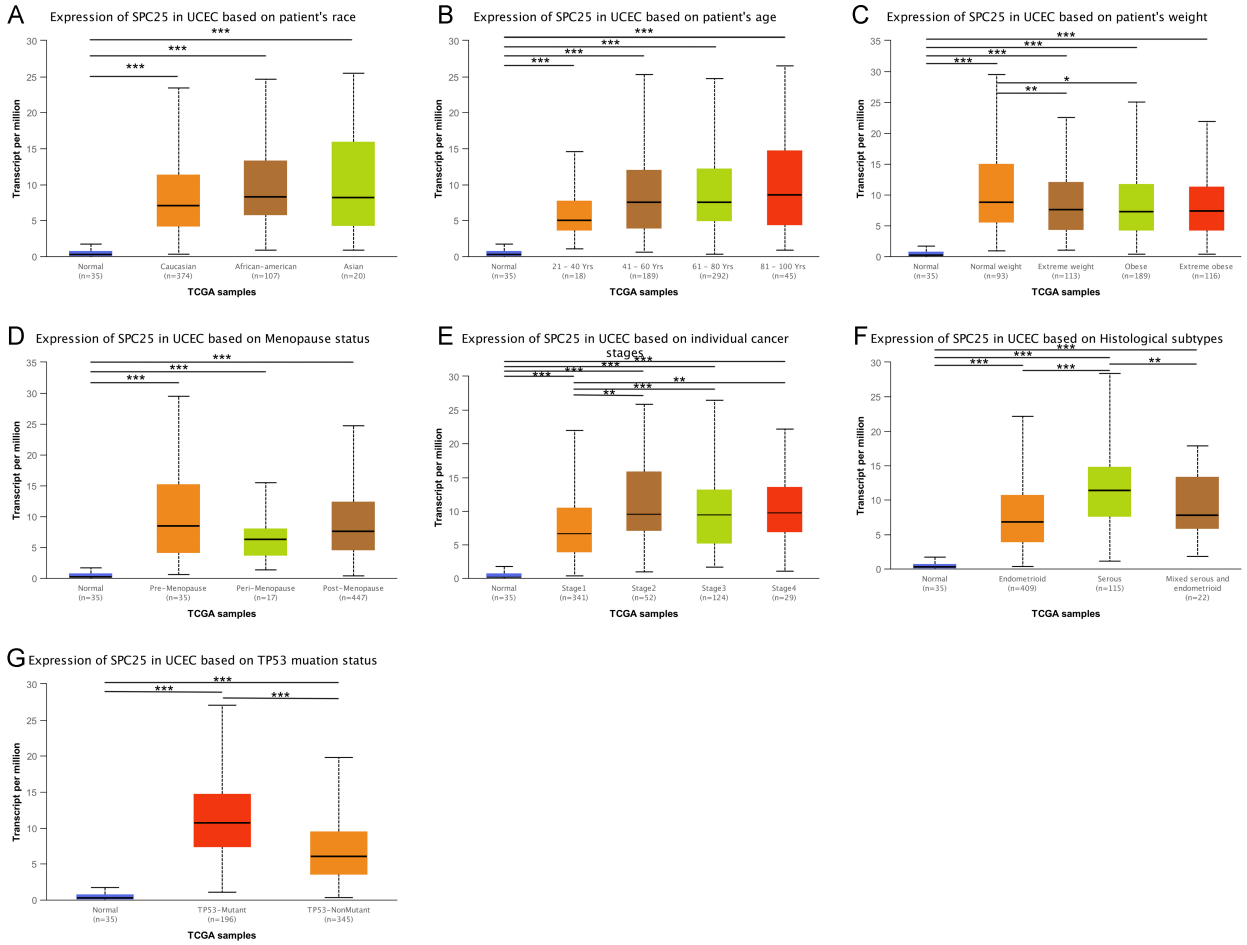

Fig. 3. Associations between *SPC25* expression and different clinical characteristics in UCEC analyzed by the UALCAN database (A–G). (A) Patient's race; (B) Patient's age; (C) Patient's weight; (D) Menopause status; (E) Individual cancer stages; (F) Histological subtypes; (G) TP53 mutation status. *$p < 0.05$; **$p < 0.01$; ***$p < 0.001$. TCGA, the cancer genome atlas.

with various clinical features and discovered that *SPC25* expression was substantially varied in race, age, weight, menopause status, stage, histological subtypes, and TP53 mutation status of UCEC (Fig. 3A–G, respectively).

3.3 SPC25 Prognostic Value in UCEC

The area under the ROC curve was 0.986 (>0.9), demonstrating *SPC25*'s excellent accuracy in predicting UCEC and its positive diagnostic impact on this condition (Fig. 4A). Additionally, we discovered that the OS, RFS, DSS, and PFI of UCEC patients with high *SPC25* expression were worse (Fig. 4B–F). So we then looked at the relationships between *SPC25* and prognosis (OS, DSS, and PFI) in several UCEC clinical subgroups. Increased *SPC25* expression was associated with a lower OS in most clinical subgroups, including subgroup of race (white), age >60, height >160, weight >80, body mass index (BMI) >30, menopause status (post), clinical stage (stage III), histological type (endometrioid), diabetes (No), hormones therapy (No), radiation therapy (No), and surgical approach (minimally invasive) (Fig. 5A–L, respectively). For DSS, increased *SPC25* expression was associated with a lower DSS in subgroup of race (white), age >60, height >160, clinical stage (stage III), tumor invasion (%) (≥50), diabetes (No), weight >80, BMI >30, menopause status (post), hormones therapy (No), radiation therapy (No), surgical approach (minimally invasive), residual tumor (R0), and primary therapy outcome (CR) (Fig. 6A–N, respectively). For PFI, increased *SPC25* expression was associated with a lower PFI in subgroup of race (white), age >60, height >160, weight ≤80, weight >80, BMI >30, menopause status (post), clinical stage (stage III), tumor invasion (%) (≥50), diabetes (No), and radiation therapy (No) (Fig. 7A–K, respectively).

3.4 SPC25 Coexpression Network Correlated with the Cell Cycle

Then, utilizing the LinkedOmics, STRING, Draw Venn Diagram, PathCards, and Xiantao Academic online tools, we investigated the *SPC25* coexpression network to confirm *SPC25*'s possible role in tumor tissue, using UCEC as an example to demonstrate its possible impact.

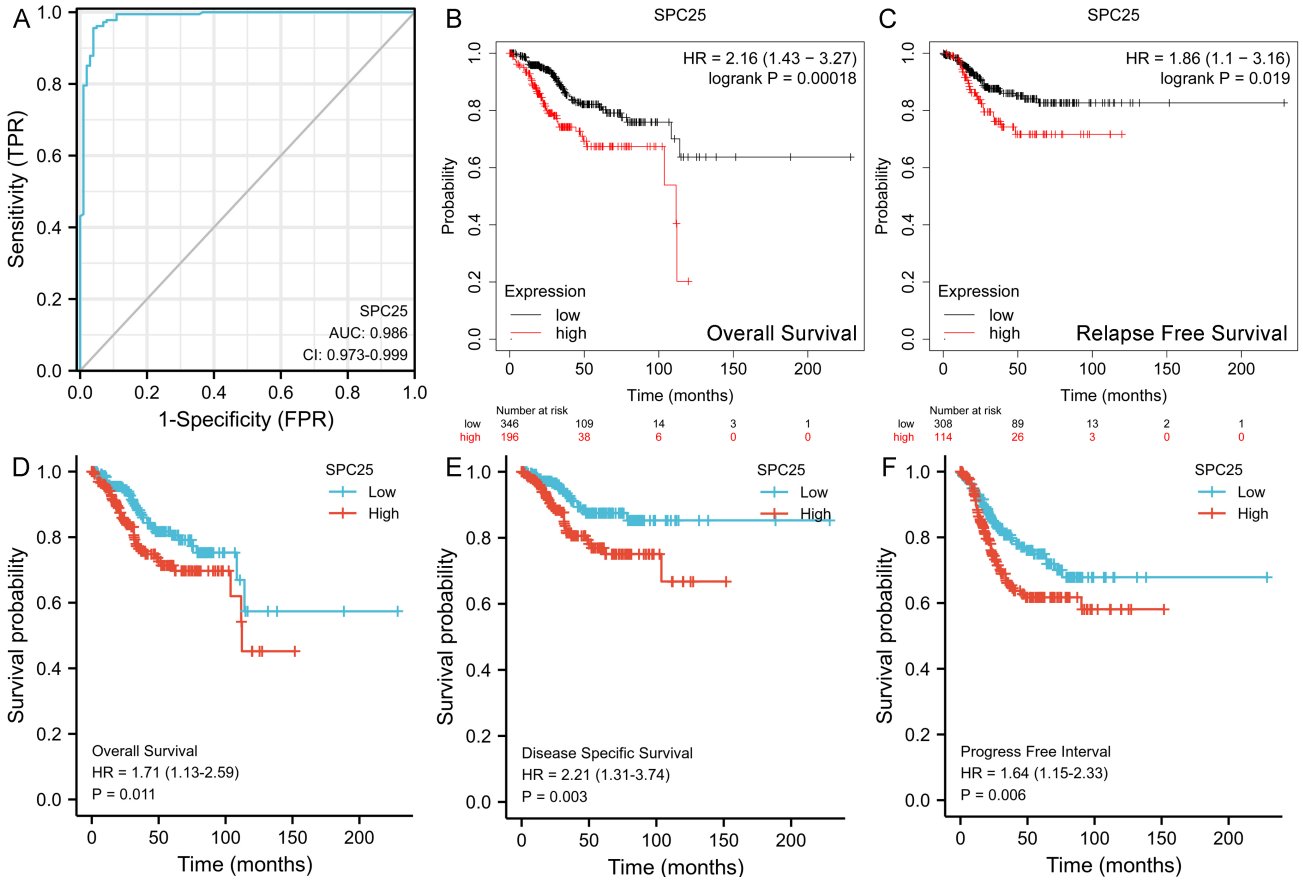

Fig. 4. *SPC25*'s prognostic value in UCEC. (A) The receiver operating characteristic (ROC) curve reflected the *SPC25*'s diagnostic ability for UCEC; (B,C) Kaplan-Meier (KM) plots showing *SPC25*'s influence on poorer overall survival (OS) (B) and recurrence free survival (RFS) (C) in UCEC patients from the Kaplan-Meier Plotter website; (D–F) KM plots showing *SPC25*'s influence on OS (D), disease-specific survival (DSS) (E), and progress free interval (PFI) (F) in UCEC patients from the Xiantao Academic website. All *p* values were less than 0.05. FPR, false positive rate.

In UCEC, 1981 genes (dark red dots) were substantially positively connected to *SPC25*, whereas 2213 genes (dark green dots) were inversely proportional to *SPC25* (FDR, 0.01) (Fig. 8A). In addition, **Supplementary Table 1** included a list of all *SPC25* coexpressed genes. The top 50 genes that were positively and negatively linked with *SPC25* were exhibited on heat maps (Fig. 9A,C). The top 10 genes that were positively and negatively linked with *SPC25* were exhibited on scatter diagrams (Fig. 9B,D). *KIFC1* (kinesin family member C1), *TPX2* (TPX2 microtubule nucleation factor), *HJURP* (Holliday junction recognition protein), *LRRC48* (DRC3, dynein regulatory complex subunit 3), *SLC46A2* (solute carrier family 46 member 2), and *ZDHHC1* (zinc finger DHHC-type containing 1) had the strongest association with *SPC25* expression ($r = 8.498 \times 10^{-1}$, 8.417×10^{-1}, 8.307×10^{-1}, -5.635×10^{-1}, -5.497×10^{-1}, -5.489×10^{-1}, $p = 2.819 \times 10^{-50}$, 1.921×10^{-48}, 3.909×10^{-46}, 3.890×10^{-16}, 2.774×10^{-15}, 3.104×10^{-15}, and FDR = 2.805×10^{-46}, 1.274×10^{-44}, 1.945×10^{-42}, 3.669×10^{-14}, 2.421×10^{-13}, 2.652×10^{-13}, respectively).

The GO_BP and KEGG analysis of *SPC25* coexpressed genes were then determined using GSEA. We looked into the GO biological process categories and discovered that *SPC25* and its coexpressed genes were mostly involved in chromosome segregation, DNA replication, cell cycle checkpoint, spindle organization, and negative regulation of cell cycle process. Then, we carried out KEGG pathway analysis, which revealed that *SPC25* coexpressed genes were prominent in Cell cycle, Spliceosome, DNA replication, RNA transport, and Oocyte meiosis (Fig. 10 and **Supplementary Table 2**).

We obtained 29 SPC25 interacting proteins from STRING, and Venn diagram showed that *BUB1* and *NDC80* were both SPC25 interacting proteins and *SPC25* coexpressed genes (Fig. 8B,C). The heat map showed that *SPC25* was significantly correlated with the expression of genes in the cell cycle pathway network, which further indicated that *SPC25* was highly likely to participate in the biological processes and signal transduction pathways of cell cycle, DNA replication, and chromosome separation (Fig. 11 and **Supplementary Table 3**).

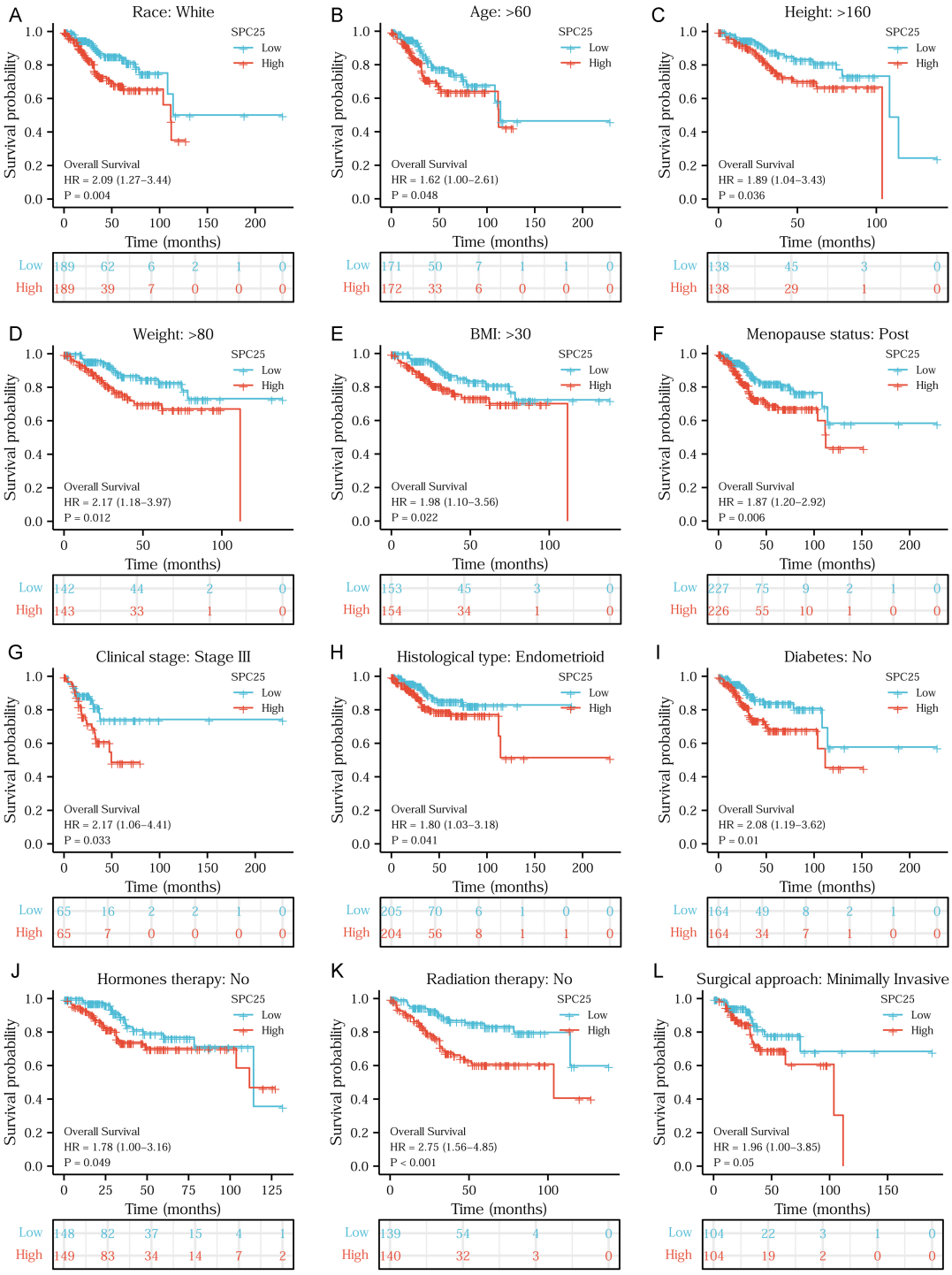

Fig. 5. Relationships between the OS and *SPC25* expression in various UCEC clinical subgroups. (A) Race: White; (B) Age >60; (C) Height: >160; (D) Weight >80; (E) body mass index (BMI) >30; (F) Menopause status: Post; (G) Clinical stage: Stage III; (H) Histological type: Endometrioid; (I) Diabetes: No; (J) Hormones therapy: No; (K) Radiation therapy: No; (L) Surgical approach: Minimally Invasive. All *p* values were less than 0.05.

3.5 Methylation Status of the SPC25 Gene Was Connected with the Prognosis of UCEC Patients

In contrast to normal samples, UCEC tissues had considerably reduced levels of *SPC25* DNA methylation (Fig. 12A). The higher the tumor grade, the lower the methylation degree (Fig. 12B). Utilizing the MetSurv tool, it was possible to examine the *SPC25* gene's DNA methylation levels as well as its CpG islands' prognostic significance. The outcomes revealed 12 methylated CpG islands: cg05868191, cg06350524, cg06580318,

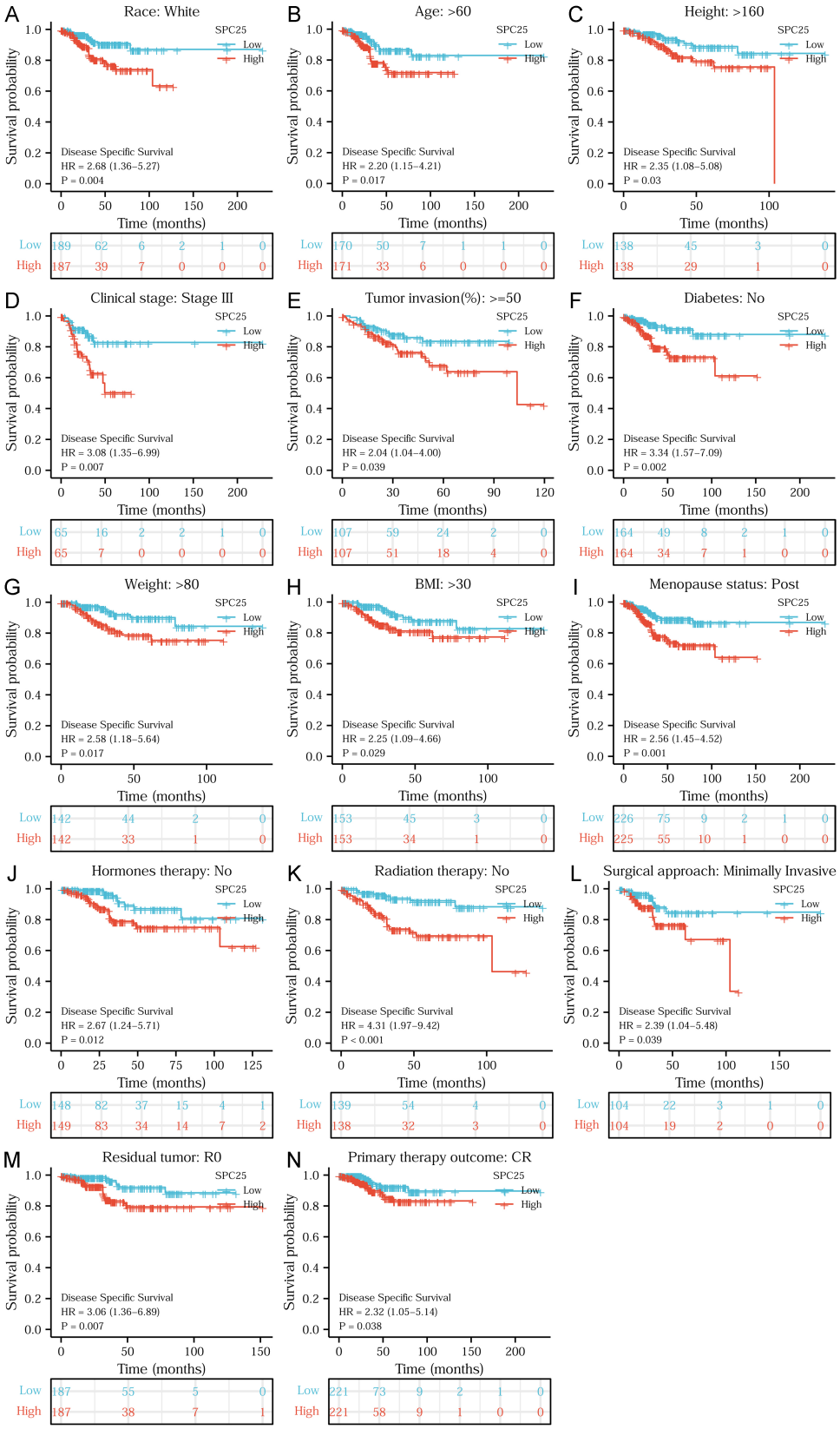

Fig. 6. Associations between *SPC25* expression and the DSS in different clinical subgroups of UCEC. (A) Race: White; (B) Age >60; (C) Height: >160; (D) Clinical stage: Stage III; (E) Tumor invasion (%): ≥50%; (F) Diabetes: No; (G) Weight >80; (H) BMI >30; (I) Menopause status: Post; (J) Hormones therapy: No; (K) Radiation therapy: No; (L) Surgical approach: Minimally Invasive; (M) Residual tumor: no residual tumor (R0); (N) Primary therapy outcome: CR. All *p* values were less than 0.05.

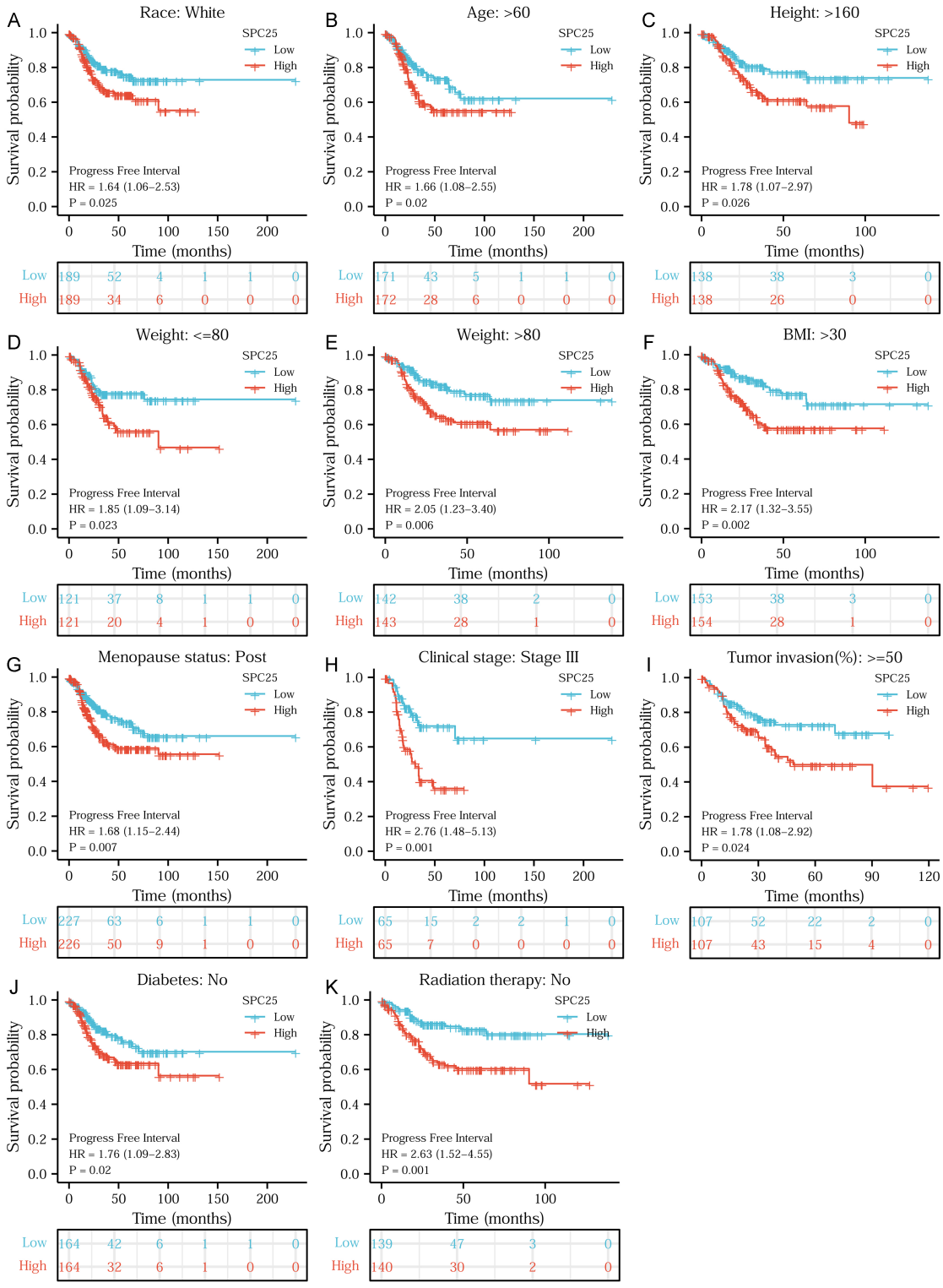

Fig. 7. Associations between *SPC25* expression and the PFI in different clinical subgroups of UCEC. (A) Race: White; (B) Age >60; (C) Height: >160; (D) Weight ≤80; (E) Weight >80; (F) BMI >30; (G) Menopause status: Post; (H) Clinical stage: Stage III; (I) Tumor invasion (%): ≥50%; (J) Diabetes: No; (K) Radiation therapy: No. All *p* values were less than 0.05.

cg13605690, cg22278106, cg15237047, cg04949346, cg17942426, cg07224215, cg20609092, cg06971765, and cg14465028 among which only cg05868191 was hypermethylated (Fig. 12C). Furthermore, methylation levels of four CpG islands, namely, cg22278106, cg15237047, cg07224215, and cg20609092 were associated with the prognosis of UCEC patients ($p < 0.05$) (Fig. 12D–G and Table 1). Specifically, when compared to individuals with

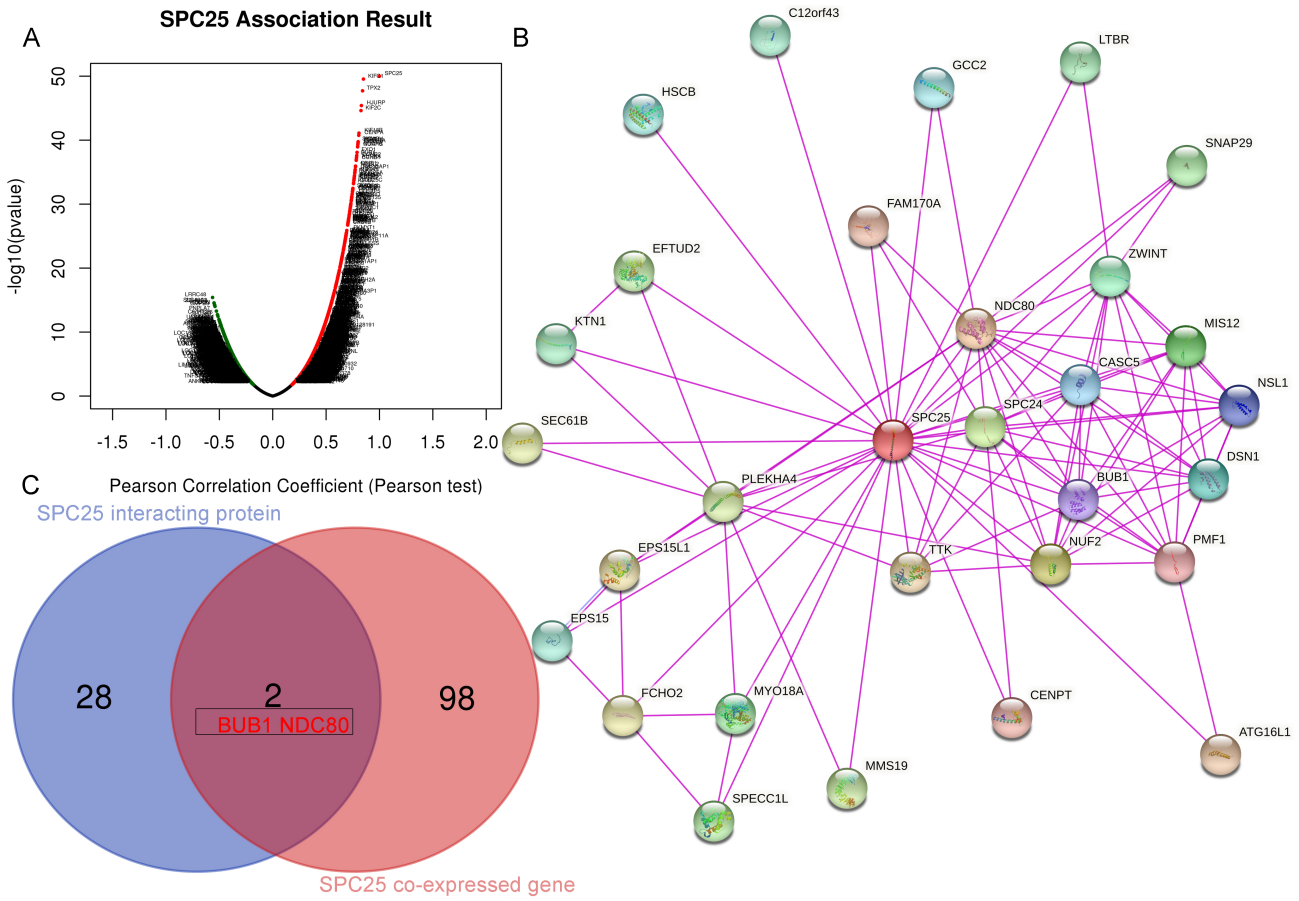

Fig. 8. *SPC25*'s co-expressed genes and interacting proteins. (A) Volcano plot obtained from the LinkedOmics database showing *SPC25*'s co-expressed genes tested by Pearson test in UCEC cohort; (B) Protein-protein interaction network of SPC25 obtained from the STRING online tool; (C) Venn diagram showed the intersection result of *SPC25*'s co-expressed genes and interacting proteins.

greater methylation levels in *SPC25* CpG sites, UCEC patients with lower levels of *SPC25* methylation in the cg22278106 and cg15237047 CpG islands had a better OS rate. Conversely, as opposed to individuals with greater levels of CpG methylation in *SPC25*, UCEC patients with lower levels of *SPC25* methylation in the cg07224215 and cg20609092 CpG islands had a worse OS rate.

3.6 SPC25 was Linked to Infiltration Levels and Checkpoint-Related Genes of Immune Cells in UCEC

Considering that tumor-infiltrated lymphocyte cells play a significant role in cancer development and affect patient prognosis and that *SPC25* might be a potential oncogene in UCEC, we next examined whether *SPC25* was related to the immune infiltration degree in UCEC. Our finding suggested that mRNA expression levels of *SPC25* had a significantly positive association with Th2 cells, T helper cells, Tgd, Tcm, and Th1 cells. On the contrary, *SPC25* expression was negatively correlated with Tfh, T cells, Treg, CTL, Th17 cells, mast cells, NK cells, eosinophils, neutrophils, iDC, pDC, and NK CD56bright cells (Fig. 13A–N). We collected these immune cell s' markers from the TISIDB website, and investigated the expression association between *SPC25* and these markers using the Xiantao academic web, which further verified the results above **(Supplementary Table 4)**. Furthermore, we found that the expression levels of *SPC25* had a significant correlation with immune checkpoints in UCEC, such as *TNFRSF14*, *TNFSF4*, *CD244*, *LAG3*, *ICOS*, *CD40LG*, *ADORA2A*, *CD276*, *CD80*, *LGALS9*, *TNFSF14*, *ICOSLG*, *TMIGD2*, *PDCD1LG2*, *HHLA2*, *TNFSF18*, *TNFSF9*, *TNFRSF8*, *CD27*, *TNFRSF25*, *VSIR*, *TNFRSF4*, *CD40*, *TNFRSF18*, and *CD274* (Fig. 13O).

3.7 SPC25 was Correlated with Immunomodulators and Chemokines in UCEC

SPC25 expression was obviously negatively correlated with immune stimulators, such as *C10orf54*, *CD27*, *CD28*, *CD40LG*, *CD48*, *CD70*, *CD276*, *CXCL12*, *HHLA2*, *IL6R*, *KLRC1*, *KLRK1*, *NT5E*, *RAET1E*, *TMEM173*, *TMIGD2*, *TNFRSF4*, *TNFRSF13B*, *TNFRSF14*, *TNFRSF17*, *TNFRSF18*, *TNFRSF25*, *TNFSF13*, *TNFSF14*, and *TNFSF15* **(Supplementary Fig. 1A)**. On the contrary, the expression of *SPC25* was considerably positively associated with immune inhibitors, including *IL10*, *LAG3*, *PDCD1LG2*, and *TGFBR1* **(Supplementary Fig.**

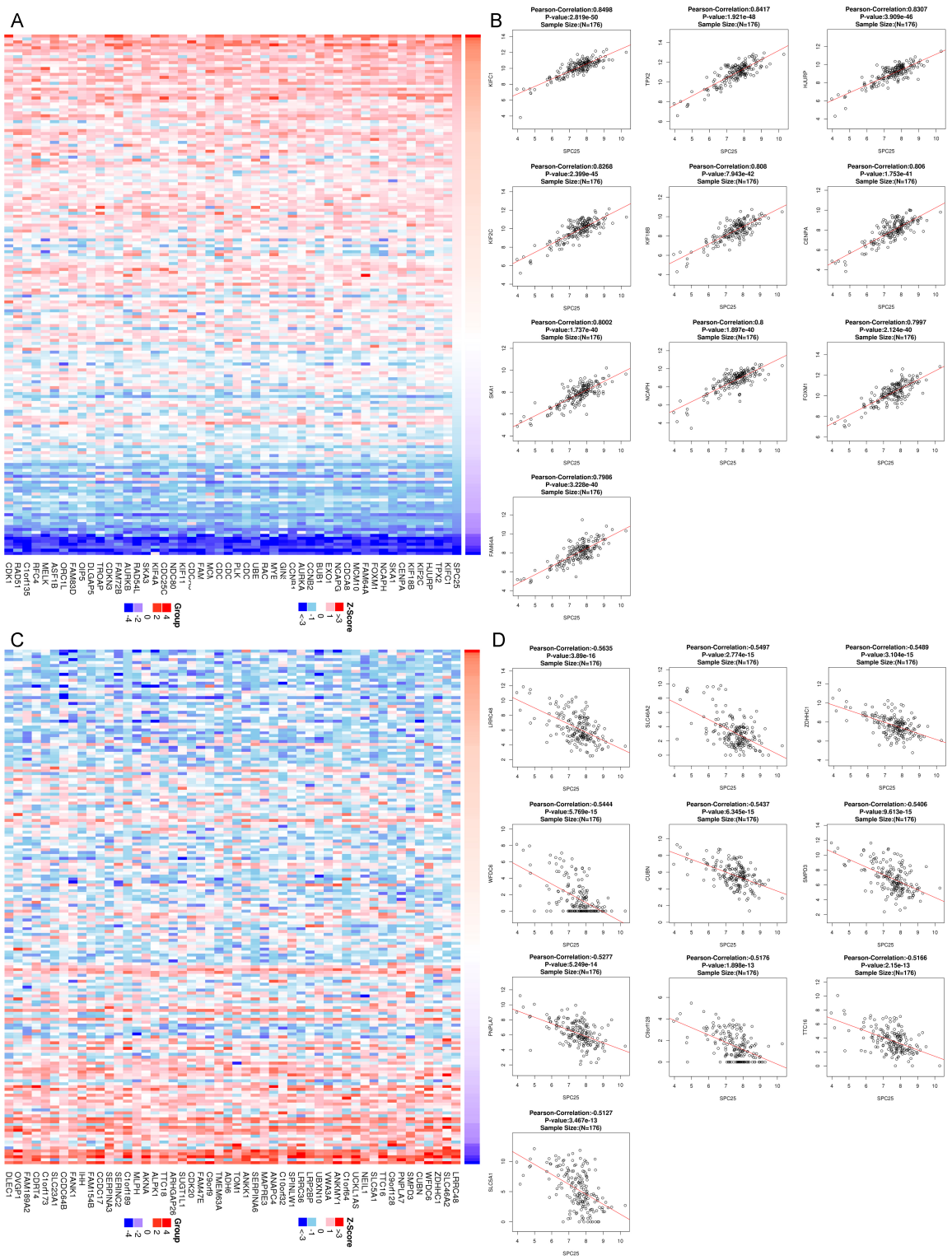

Fig. 9. *SPC25*'s positively and negatively co-expressed genes in UCEC analyzed by the LinkedOmics database. (A,C) the top 50 positively co-expressed (A) and negatively co-expressed (C) genes of *SPC25* shown in heat maps; (B,D) the top 10 positively co-expressed (B) and negatively co-expressed (D) genes of *SPC25* represented by scatter plots. A *p* value of less than 0.05 was considered statistically significant.

1B). *SPC25* expression was markedly negatively related to chemokines such as *CCL14*, *CCL15*, *CCL17*, *CCL19*, *CCL20*, *CCL21*, *CCL22*, *CCL23*, *CCL24*, *CX3CL1*, *CXCL2*, *CXCL3*, *CXCL5*, *CXCL12*, *CXCL14*, *CXCL17*, *XCL1*, and *XCL2* **(Supplementary Fig. 1C)**. Meanwhile, the expression of *SPC25* was distinctly negatively con-

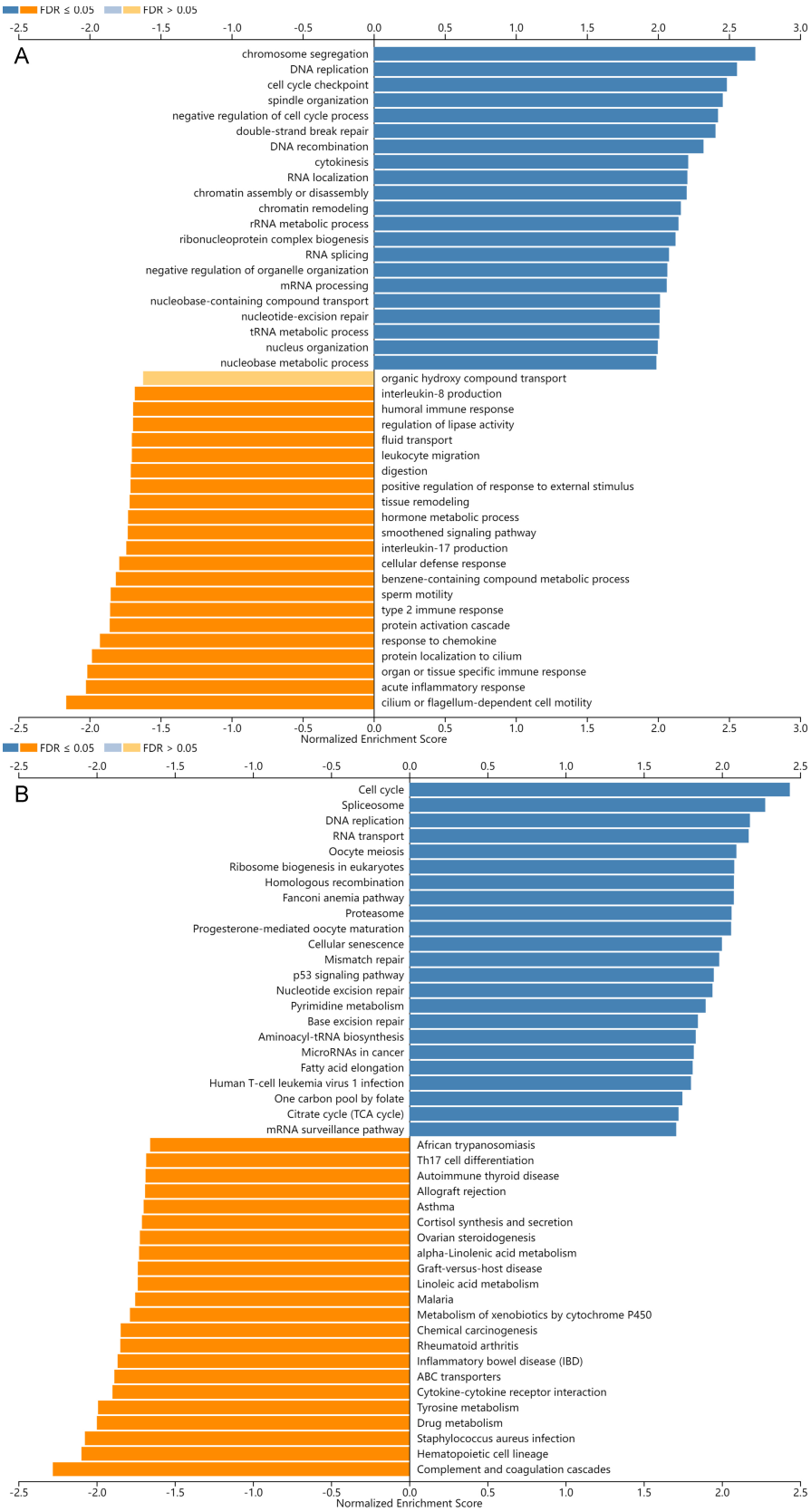

Fig. 10. *SPC25*'s gene set enrichment analysis (GSEA) analysis in UCEC cohort analyzed by the LinkedOmics database. (A) Bar chart of *SPC25*'s gene ontology biological process (GO_BP) (biological process) analysis; (B) Bar chart of *SPC25*'s kyoto encyclopedia of genes and genomes (KEGG) pathways. A false discovery rate (FDR) value of 0.05 or less was considered statistically significant.

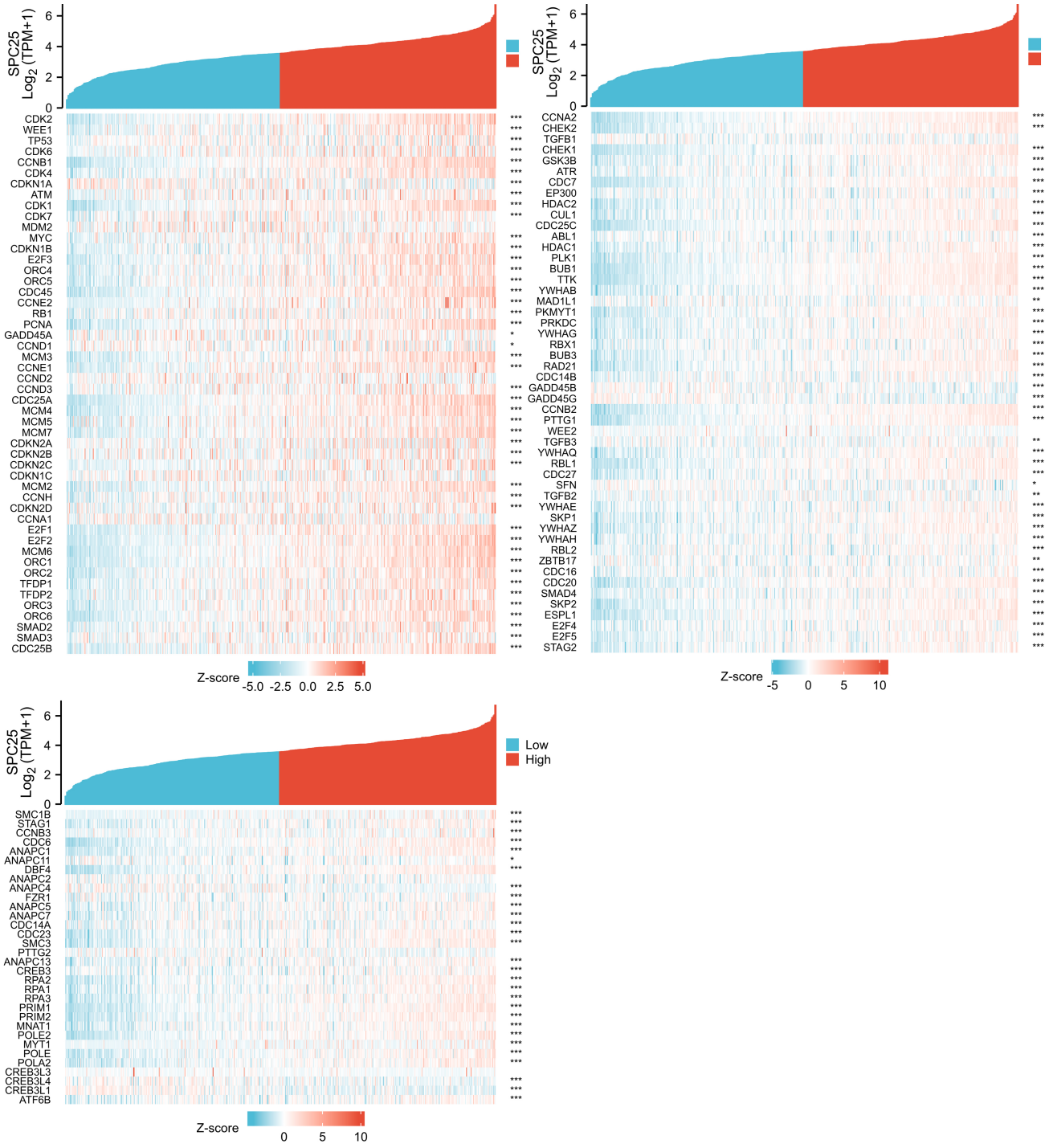

Fig. 11. The heat maps obtained from the Xiantao Academic web showing the correlation between *SPC25* and the genes in the cell cycle pathway network queried from the PathCards website in UCEC. *, $p < 0.05$; **, $p < 0.01$; ***, $p < 0.001$.

nected with chemokine receptors, including *CCR2*, *CCR3*, *CCR4*, *CCR5*, *CCR6*, *CCR7*, *CCR10*, *CX3CR1*, *CXCR1*, *CXCR2*, *CXCR2*, *CXCR5*, and *CXCR6* **(Supplementary Fig. 1D)**. These data provided credence to the hypothesis that *SPC25* could operate as an immunoregulatory component in UCEC.

3.8 SPC25 Methylation was Associated with Immunosuppressive Status in UCEC

As shown in the previous research, *SPC25* methylation correlated with prognosis in UCEC. To clarify the role of *SPC25* methylation in the progression of UCEC, we assessed the relationship of *SPC25* methylation with immune infiltration utilizing the TISIDB platform. The result revealed that *SPC25*'s methylation status was posi-

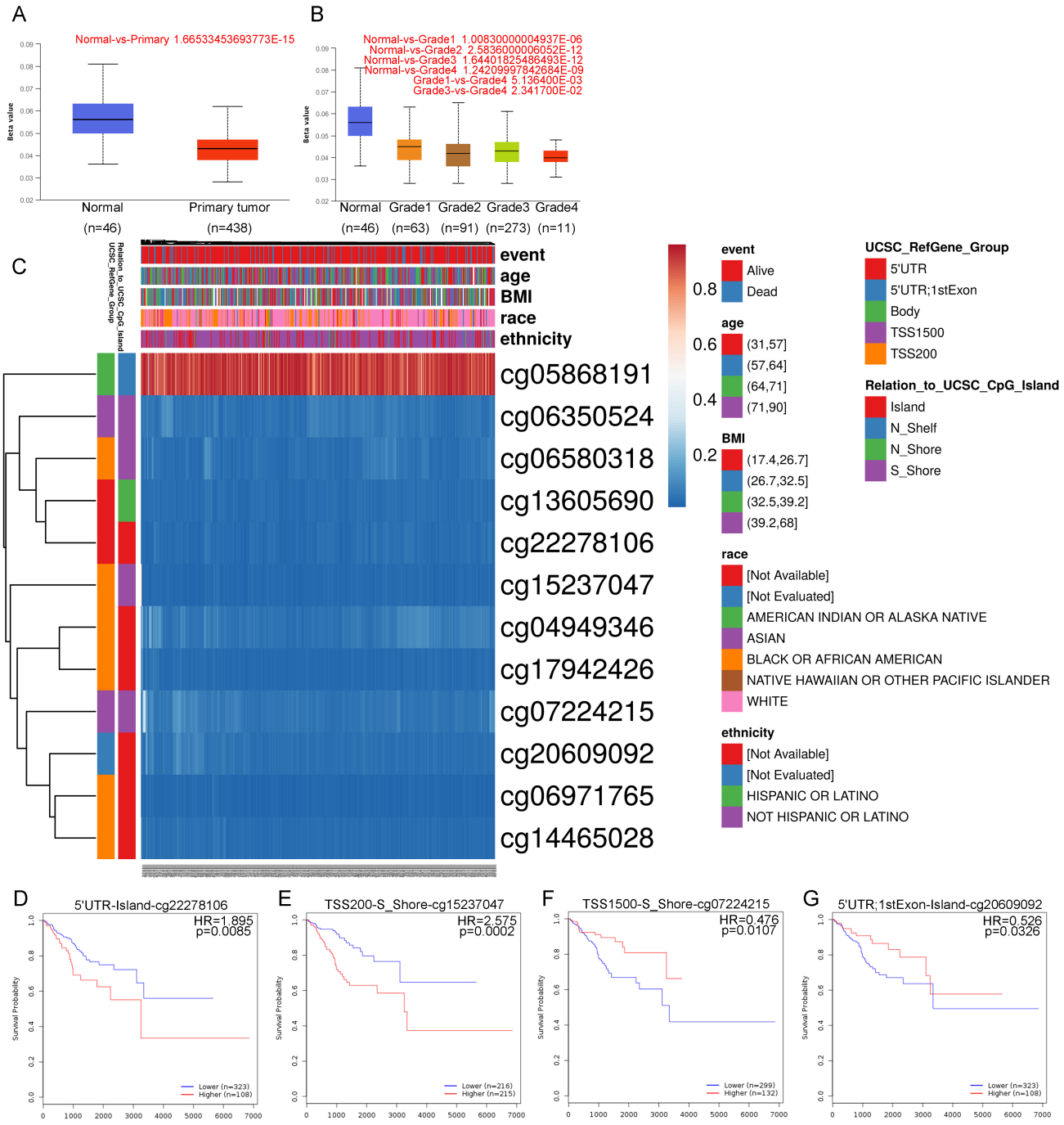

Fig. 12. DNA methylation levels in the *SPC25* gene were associated with the prognosis of UCEC patients. (A) Promoter methylation level of *SPC25* in normal tissues and primary UCEC tissues by the UALCAN database. (B) Promoter methylation level of *SPC25* of various tumor grades in UCEC tissues by the UALCAN database. (C) The heat map of DNA methylation at CpG sites in the *SPC25* gene by the MethSurv database. (D–G) The association between methylation levels of four CpG islands of the *SPC25* gene and OS of UCEC patients: (D) cg22278106, (E) cg15237047, (F) cg07224215, and (G) cg20609092.

tively correlated with the infiltration level of Act-B, Act-CD8, Eosinophil, iDC, Imm-B, Macrophage, Mast, MDSC, Monocyte, Neutrophil, NK, NKT, pDC, Tcm-CD4, Tem-CD8, Tfh, Th1, and Th17 **(Supplementary Fig. 2A)**. Similarly, the methylation status of *SPC25* was positively associated with immune stimulators, such as *CD27*, *CD28*, *CD40LG*, *CD48*, *CD86*, *CXCL12*, *ENTPD1*, *ICOS*, *IL2RA*, *KLRC1*, *KLRK1*, *LTA*, *NT5E*, *RAET1E*, *TMIGD2*, *TNFRSF13B*, *TNFRSF14*, *TNFRSF17*, *TNFRSF18*, and *TNFSF14* **(Supplementary Fig. 2B)**, while being negatively related to immune inhibitors, such as *PVRL2* **(Supplementary Fig. 2C)**. *SPC25*'s methylation status was

Table 1. Effects of DNA methylation levels in the CpG sites of the *SPC25* gene on the prognosis of UCEC patients.

CpG island	HR	CI	*p* value
Body-N_Shelf-cg05868191	0.651	(0.397; 1.068)	0.088924245
TSS1500-S_Shore-cg06350524	1.586	(0.972; 2.587)	0.064688207
TSS200-S_Shore-cg06580318	1.491	(0.844; 2.632)	0.168508099
5′UTR-N_Shore-cg13605690	1.828	(0.96; 3.482)	0.066421999
5′UTR-Island-cg22278106	**1.895**	**(1.177; 3.049)**	**0.008501209**
TSS200-S_Shore-cg15237047	**2.575**	**(1.569; 4.227)**	**0.000182488**
TSS200-Island-cg04949346	1.294	(0.814; 2.056)	0.276525993
TSS200-Island-cg17942426	0.571	(0.321; 1.018)	0.057476853
TSS1500-S_Shore-cg07224215	**0.476**	**(0.269; 0.842)**	**0.010685551**
5′UTR;1stExon-Island-cg20609092	**0.526**	**(0.291; 0.948)**	**0.032599855**
TSS200-Island-cg06971765	0.818	(0.488; 1.369)	0.443815502
TSS200-Island-cg14465028	0.64	(0.357; 1.148)	0.134276835

HR, hazard ratio; CI, confidence interval.

Notes: Bold in the table above indicated that the *p* value was less than 0.05, and the difference was statistically significant.

also positively connected with chemokines and receptors, such as *CCL4*, *CCL5*, *CCL14*, *CCL15*, *CCL17*, *CCL19*, *CCL21*, *CCL22*, *CCL23*, *CCL24*, *CXCL2*, *CXCL3*, *CXCL5*, *CXCL12*, *CXCL14*, *CXCL17*, *XCL2*, *CCR2*, *CCR4*, *CCR5*, *CCR7*, *CXCR1*, *CXCR2*, *CXCR3*, *CXCR5*, and *CXCR6* **(Supplementary Fig. 2D,E)**. These findings showed that *SPC25*'s methylation status was adversely correlated with immunosuppressive state of UCEC.

4. Discussion

SPC25 is an significant kinetochore component that plays an indispensable role in normal mitosis. The lack of SPC25 results in mitotic abnormality, followed cell death and the loss of SPC25 also causes multiple spindle aberrations, including spindle elongation, multipolarity, and fracture. In the case where there is no SPC25, MAD1 and HEC1 fail to correctly localize at the kinetochores during mitosis [38].

Up to now, some scholars have published some research results on *SPC25*. For instance, *SPC25* could serve as a potential tumor-promoting factor, a metastasis promoter, a useful prognostic indicator, and a new therapy target for HCC. *SPC25* mRNA expression was shown to be elevated in HCC, and greater levels of *SPC25* expression were linked to a worse prognosis. *SPC25* accelerated the cell cycle, allowing HCC cells to proliferate in vitro and tumor growth in vivo. In vitro, knocking down or silencing of *SPC25* led to a considerable reduction in HCC cell proliferation and metastasis, a marked inhibition of invasion and migration, and increased protein level of p53 pathway components. *SPC25* might promote proliferation and metastasis of HCC via p53 or via activating the FAK/PI3K/AKT signaling pathway through ITGB4 [10–13].

SPC25 was considerably enhanced in lung adenocarcinoma (LUAD) tissue relative to normal lung tissue, increased cancer stem-like cell (CSC) properties and A549 cell invasion, and was an independent predictive factor for LUAD patients' poor OS and recurrence free survival (RFS). Additionally, lung cancer cell proliferation requires SPC25 homologs expressed in extracellular matrix (ECM) stiffening. In idiopathic pulmonary fibrosis (IPF-LC), because *CADM1* and *SPC25* were implicated in transforming growth factor-beta 1 (TGF-beta 1) signaling, gene mutations in these two genes resulted in reduced *CADM1* expression and increased *SPC25* expression in lung cancer cells, revealing TGF-beta 1-induced epithelial-mesenchymal transition and cell proliferation [14–16].

In PCa, *SPC25* was shown to be highly elevated. *SPC25* knockdown decreased proliferation and accelerated apoptosis in PCa cells, resulting in a drop in the number of S phase cells and an increase in the number of G2/M phase cells. *SPC25* also has several functional functions in regulating cell proliferation, apoptosis, invasion, transforming growth factor-beta signaling, and SUMOylation pathways in PCa, according to bioinformatic study. *SPC25* was upregulated in advanced PCa, and PrC patients with higher *SPC25* have lower OS than those with lower *SPC25*. SPC25+ cells developed considerably more tumorspheres in vitro culture than SPC25- cells, seemed to be more resistant to docetaxel-induced cell apoptosis, and created bigger tumors with a greater frequency after repeated adoptive transplantation than SPC25- cells [17,18].

SPC25 level was higher in more aggressive BC cell subtypes, and BC patients had a worse prognosis when *SPC25* was expressed to a greater extent. *SPC25* increased BC cell proliferation, as evidenced by colony formation and CCK-8 experiment. In addition, treatment with DNA methyltransferase inhibitors and transcription factor inhibitors targeting *SPC25* might improve prognosis in BC patients. The combination of the DNMT inhibitor 5-azacytidine and the HDAC inhibitor butyrate significantly reduced the abundance of CSC, blocked CSC tumori-

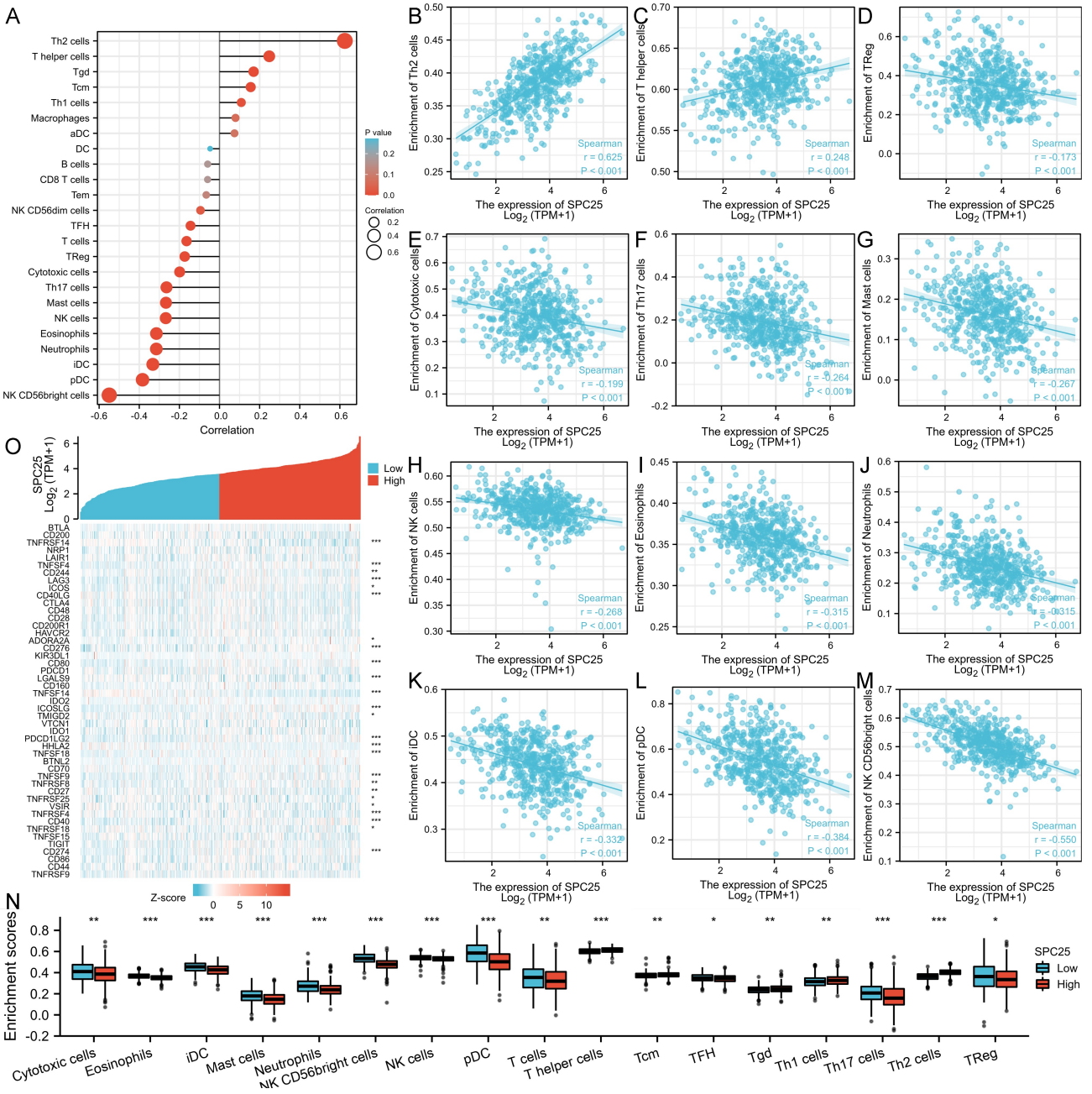

Fig. 13. Correlation analysis of *SPC25*'s expression and immune cells' infiltration level as well as immune checkpoints in UCEC conducted in the Xiantao Academic online tool. (A–N) The correlation between *SPC25*'s expression and infiltration level of immune cells. (O) Expression correlation analysis of *SPC25* and immune checkpoint-related genes. *$p < 0.05$; **$p < 0.01$; ***, $p < 0.001$.

genicity, attenuated breast tumor growth, and improved OS in the MMTV-Neu-Tg mouse model, likely because growth-promoting signaling molecules such RAD51AP1 and SPC25 were prevented when chromatin modifiers were inhibited [19].

Specific depletion of *SPC25* in microglia might prevent Alzheimer's disease (AD) development by inhibiting microglia outgrowth [20]. During meiosis, *SPC25* is needed for chromosomal alignment, spindle formation, and appropriate spindle checkpoint signaling [21].

However, as far as we know, there is currently no research that can fully assess the importance of *SPC25* in UCEC. Therefore we made an effort to fill the research gap of *SPC25* in UCEC. In our findings, *SPC25* mRNA and protein expression were shown to be elevated in UCEC tissues and substantially connected with clinical stage, histologic grade, histological type, radiation therapy, tumor invasion, weight, primary therapy outcome, molecular subtype, immune subtype, and *TP53* muation status in UCEC. Taken together, *SPC25* was upregulated in UCEC and might act as a pivotal player in the carcinogenesis of UCEC.

Following that, we observed that increased *SPC25* expression could lead to poorer OS, RFS, DSS, and PFI of UCEC patients. In addition, elevated *SPC25* was associated with poorer OS, DSS, and PFI in a number of clinical subgroups of UCEC, yet cause a worse all of the OS, DSS, and PFI only in race (white), age >60, height >160, weight >80, BMI >30, menopause status (post), clinical stage (stage III), diabetes (No), and radiation therapy (No). It is of great importance that for the first time, we examined the relationships between *SPC25* expression and various prognostic (OS, DSS, and PFI) in several clinical subgroups of UCEC.

SPC25 coexpression network analyses in UCEC pointed out that *SPC25* regulated the cell cycle of tumor cells in the TME, which was in line with findings from other studies.

Tumorigenesis is significantly influenced by DNA methylation, a common epigenetic mechanism. Changes in the methylation status of several genes have been connected to the initiation, growth, and advancement of various malignancies [39,40]. Consequently, we investigated the promoter methylation status of *SPC25* in UCEC utilizing the UALCAN database. We discovered that the DNA methylation levels of *SPC25* in cancer tissues were noticeably lower than those in healthy samples, indicating that *SPC25*'s overexpression in UCEC was caused by a low degree of promoter methylation status. Our research also showed that high-grade UCEC commonly had lower methylation levels of *SPC25*, which might indicate that the pattern alteration of *SPC25* methylation encouraged the advancement of UCEC. Besides, we looked at the association between the *SPC25* gene's methylation levels and the prognosis of UCEC patients. UCEC patients who had hypomethylation at two CpG sites, including cg22278106 and cg15237047, had an excellent OS rate. However, UCEC patients' poor OS was linked to the hypomethylation of two CpG sites, namely cg07224215 and cg20609092. All four of these CpG sites saw a reduction in methylation. Our research yielded two contradicting results. Our hypothesis was that hypomeylation of the final two CpG sites had a greater impact on the prognosis of UCEC patients than did the first two. This suggested that the latter two CpG sites could be future therapeutic targets for reducing *SPC25* expression and improving the UCEC patients' prognosis. In general, we discovered that the majority of methylation sites in the DNA sequences of *SPC25* were hypomethylated in UCEC, and the degree of methylation was connected with patient outcomes. These findings revealed that *SPC25* methylation levels functioned as an efficient predictive biomarker for UCEC, suggesting that *SPC25* might play a crucial role in tumor progression.

Initial theories presupposed that an effective immune response might have an antitumor impact, but cancer cells have evolved a number of mechanisms, such as impaired antigen presentation and the recruitment of immunosuppressive cells, which encourage tumors to avoid the attack of immune cells. According to earlier research, immune infiltration can have an impact on a patient's prognosis, and tumor-infiltrating lymphocyte grade is an independent predictor of sentinel lymph node status in patients with tumors [41]. In this study, *SPC25* was shown to be substantially expressed in UCEC and linked to a poor outcome for those patients with UCEC. We also found that *SPC25* expression had a clearly positive association with Th2 cells, T helper cells, and Th1 cells. Conversely, *SPC25* was visibly negatively correlated with T cells, CTL, NK cells, neutrophils, iDC, and pDC.

The T helper cell-expressed TGF is a key player in the resistance mechanisms against cancer immunotherapy. An efficient tissue-level cancer defense response is elicited by targeted TGF- signaling inhibition in helper T cells, which can serve as a foundation for therapeutics focused on the cancer environment [42]. Th2 cells can turn macrophages into tumor-promoting cells and change the immune response from a cytotoxic to a supportive function when they are present in the TME [43]. Myeloma cell growth and function were markedly suppressed by CTL and Th1 cells, but Th2 cells promoted myeloma cell proliferation and cytokine secretion. In multiple myeloma, CTL and Th1 responses are advantageous and will result in tumor elimination after immunotherapy. In contrast, a Th2 response offers little protection and could even hasten the growth of tumors in vivo [44]. Effector cells of the adaptive immune system are $CD8^+$ CTL cells, which precisely identify and eliminate cancer cells through apoptosis that is mediated by perforin and granzyme [45]. T cell depletion is a significant barrier to successful immunotherapy [46]. Cytotoxic lymphocytes called NK cells may obliterate stressed cells even in the absence of an antigen presentation. NK cells identify and eradicate tumor cells through "missing-self" activation (loss of healthy cell markers) or "stress-induced" activation (gain of stressed cell markers) [47]. Through triggering T cell responses against the tumor cells and directly lysing tumor cells, tumor-associated neutrophils perform a crucial anti-tumor function [48]. By cross-presenting foreign antigens, dendritic cells (DCs) play a crucial role in $CD8^+$ T cell activation and producing anti-tumor $CD8^+$ T cell immunity [49].

Most findings state that the immunogenicity of the malignancies influences the effectiveness of immune checkpoint blockade [50]. Low immunogenicity cancers tend to respond poorly to immune checkpoint-blocking treatment because T cell infiltration by malignancies is relatively small [51]. In order to preserve self-tolerance and avoid autoimmune disease, immune checkpoint molecules normally downregulate activation signals from costimulatory molecules. This method, however, might be used by tumor cells to prevent T cells from becoming activated and functioning normally, which results in T-cell depletion, tumor immune escape, and aggressive tumor growth. In our

finding, we confirmed that the *SPC25* expression levels were evidently negatively correlated with immune stimulators, such as *CD27*, *CD40LG*, *CD276*, *HHLA2*, *TMIGD2*, *TNFRSF4*, *TNFRSF14*, *TNFRSF18*, *TNFRSF25*, and *TNFSF14*. On the contrary, *SPC25* was distinctly positively associated with immune inhibitors, including *LAG3* and *PDCD1LG2*.

When it comes to the directed migration of immune cells, chemokines and their receptors are crucial [52–54]. In this study, we foud that *SPC25* was evidently negatively correlated with chemokines and their receptors: *CCL14*, *CX3CL1*, *CCR3*, *CCR4*, *CCR5*, *CCR6*, and *CX3CR1*, suggesting that High *SPC25* expression might prevent immune cells from migrating into the TME. Studies show that *CCL14*'s active form binds to *CCR1*, *CCR3*, and *CCR5* to encourage the chemotaxis of monocytes, eosinophils, and T lymphocytes [55,56]. The inflammatory receptor *CCR4* stimulates the respiratory burst and phagocytosis of macrophages [57] and regulates the differentiation of M1/M2 macrophages [58]. B cell integrin-mediated adhesion is regulated by *CCR6* [59,60]. White blood cell survival and NK cell activation are both regulated by *CX3CR1* [61], which might explain how *SPC25* regulates immune infiltration in UCEC.

These findings suggested the possibility of tumor immune escape and antitumor immunity being implicated in the *SPC25*-mediated carcinogenic mechanisms of UCEC.

Tumor immunogenicity and immune cells inside the TME will be impacted by dysregulated epigenome DNA methylation [62]. We examined the connection between *SPC25*'s methylation status and immune infiltration in order to decipher the mechanism by which *SPC25* hypomethylation promotes the progression of UCEC. Our data showed that *SPC25*'s methylation status was positively correlated with immune cells, immunostimulatory factors, chemokine and chemokine receptors while negatively connected with immunoinhibitors. This suggested that *SPC25*'s hypomethylation might contribute to immunosuppression and promote tumor progression in UCEC, which could assist to explain the *SPC25* low methylation status in high-grade UCEC tumors and poor prognosis of corresponding UCEC patients. Thus, *SPC25* methylation might serve as an indicator of cancer immune infiltration and potential predictor of UCEC patient response to immunotherapeutic drugs.

In conclusion, the mRNA and protein of *SPC25* were overexpressed in UCEC tumor tissues and associated with a variety of clinicopathological features. The expression and methylation of the *SPC25* gene were related to the prognosis of UCEC patients. *SPC25* expression levels and methylation status not only correlated with the extent to which various immune cell types were infiltrating the tumor, but also had a relationship with immunomodulators and chemokines, which might have an impact on how well immunotherapy works in UCEC patients. By modifying the expression of genes involved in cell cycle and immune response, *SPC25* controlled the course of UCEC. Therefore, *SPC25* was a valuable prognostic biomarker for UCEC, as well as a possible therapeutic target. However, further research is required to substantiate our findings.

However, even with our detailed and systematic research of *SPC25* and cross-verification using many databases, we must admit that our current research has a number of potential limitations.

On the one hand, we explored *SPC25* gene only using the public databases such as TCGA and GEO yet lacking actual clinical data. And there were variations in microarray and sequencing data from various databases, which could lead to systematic bias. Thus, further *in vivo*/*in vitro* verification experiments and follow-up multicenter, large-sample, and prospective studies should be performed to provide precise verification and high-quality evidence in order to investigate if there's a link between *SPC25* and patient survival, and to find more effective antitumor immunotherapy techniques.

On the other hand, although concluding that *SPC25* expression was significantly correlated with immune cell infiltration and cancer patients' survival, we lacked direct evidence of *SPC25* influencing prognosis despite its involvement in the regulation of immune cell infiltration. In other words, the processes by which *SPC25* regulates the immune system as well as its precise route remain unknown and need further study. We also need sufficient and accurate clinical trial data to to determine the advantages of anti-SPC25 medicines in inhibiting tumor growth or improve patient prognosis.

5. Conclusions

In conclusion, the discovery of *SPC25* investigation in UCEC might provide a integrative understanding of its crucial function in tumor promotion and suppression, and add a comprehensive analytical basis for in-depth validation of molecular biology experiments, and even for future clinical applications of cancer therapy.

Abbreviations

NDC80, nuclear division cycle 80; NUF2, NUF2 component of NDC80 kinetochore complex; SPC24, spindle pole body component 24; SPC25, spindle pole body component 25; HCC, hepatocellular carcinoma; PCa, prostate cancer; BC, breast cancer; EC, endometrial cancer; UCEC, uterine corpus endometrial carcinoma; OS, overall survival; DSS, disease-specific survival; PFI, progress free interval; TME, tumor microenvironment; GEO, gene expression omnibus; UALCAN, the university of alabama at birmingham cancer data analysis portal; TCGA, the cancer genome atlas; HPA, the human protein atlas; AUC, area under the curve; KM, kaplan-meier; GSEA, gene set enrichment analysis; IHC, immunohistochemistry; FPKM, fragments per kilobase per million; TPM, transcripts per mil-

lion; ROC, receiver operating characteristic curve; FDR, false discovery rate; TPR, True Positive Rate; RFS, recurrence free survival; GSEA, gene set enrichment analysis; GO_BP, gene ontology biological process; KEGG, kyoto encyclopedia of genes and genomes; STRING, search tool for the retrieval of interacting genes/proteins; Th1, T helper 1 cell; Th2, T helper 2 cell; Th17, T helper 17 cell; Treg, regulatory T cells; Tgd, gamma delta ($\gamma\delta$) T cells; Tcm, central memory T cells; Tfh, T follicular helper cells; CTL, cytotoxic T cell; NK cells, natural killer cells; pDC, plasmacytoid dendritic cell; iDC, immature dendritic cell; LUAD, lung adenocarcinoma; CSC, cancer stem-like cell; RFS, recurrence-free survival; ECM, extracellular matrix; IPF-LC, idiopathic pulmonary fibrosis; TGF, transforming growth factor; AD, Alzheimer's disease; DCs, dendritic cells.

Availability of Data and Materials

The datasets generated and/or analysed during the current study are available in the TCGA database (https://portal.gdc.cancer.gov/) and GEO database (https://www.ncbi.nlm.nih.gov/geo).

Author Contributions

YZG and LXL were responsible for the design of the study protocol. XX and SZ contributed to the writing of the study protocol and assisted in completing statistical analysis and picture drawing. LXL collected surgical specimens and performed Western blotting experiments. MZ downloaded the data, designed the experimental scheme, drew the pictures and performed statistical analyses. LXL performed the statistical analysis, drew the pictures and wrote the first draft of the manuscript. MZ also assisted LXL in writing the first draft. All authors contributed to manuscript revision, read, and approved the submitted version. All authors have participated sufficiently in the work and agreed to be accountable for all aspects of the work.

Ethics Approval and Consent to Participate

Approval was granted by the Ethics Committee of the Second Hospital of Lanzhou University (2023A-453). This study was performed in line with the principles of the Declaration of Helsinki. The patients/participants provided their written informed consent to participate in this study. Written informed consent was obtained from the individual(s) for the publication of any potentially identifiable images or data included in this article. TCGA and GEO databases are publicly available and written informed consent was obtained from the patients prior to data collection.

Acknowledgment

Not applicable.

Funding

This study was funded by Distant Cause Development Fund (grant number 071100136).

Conflict of Interest

The authors declare no conflict of interest.

Supplementary Material

Supplementary material associated with this article can be found, in the online version, at https://doi.org/10.31083/j.fbl2902069.

References

[1] Ustinov NB, Korshunova AV, Gudimchuk NB. Protein Complex NDC80: Properties, Functions, and Possible Role in Pathophysiology of Cell Division. Biochemistry. Biokhimiia. 2020; 85: 448–462.

[2] Alushin GM, Ramey VH, Pasqualato S, Ball DA, Grigorieff N, Musacchio A, *et al*. The Ndc80 kinetochore complex forms oligomeric arrays along microtubules. Nature. 2010; 467: 805–810.

[3] Wei RR, Schnell JR, Larsen NA, Sorger PK, Chou JJ, Harrison SC. Structure of a central component of the yeast kinetochore: the Spc24p/Spc25p globular domain. Structure (London, England: 1993). 2006; 14: 1003–1009.

[4] Alushin GM, Musinipally V, Matson D, Tooley J, Stukenberg PT, Nogales E. Multimodal microtubule binding by the Ndc80 kinetochore complex. Nature Structural & Molecular Biology. 2012; 19: 1161–1167.

[5] Meng QC, Wang HC, Song ZL, Shan ZZ, Yuan Z, Zheng Q, *et al*. Overexpression of NDC80 is correlated with prognosis of pancreatic cancer and regulates cell proliferation. American Journal of Cancer Research. 2015; 5: 1730–1740.

[6] Ju LL, Chen L, Li JH, Wang YF, Lu RJ, Bian ZL, *et al*. Effect of NDC80 in human hepatocellular carcinoma. World Journal of Gastroenterology. 2017; 23: 3675–3683.

[7] Laine LJ, Mäki-Jouppila JHE, Kutvonen E, Tiikkainen P, Nyholm TKM, Tien JF, *et al*. VTT-006, an anti-mitotic compound, binds to the Ndc80 complex and suppresses cancer cell growth *in vitro*. Oncoscience. 2021; 8: 134–153.

[8] Yan X, Huang L, Liu L, Qin H, Song Z. Nuclear division cycle 80 promotes malignant progression and predicts clinical outcome in colorectal cancer. Cancer Medicine. 2018; 7: 420–432.

[9] Gao H, Pan QY, Wang YJ, Chen QF. Impact of KMN network genes on progression and prognosis of non-small cell lung cancer. Anti-cancer Drugs. 2022; 33: e398–e408.

[10] Zhang B, Zhou Q, Xie Q, Lin X, Miao W, Wei Z, *et al*. SPC25 overexpression promotes tumor proliferation and is prognostic of poor survival in hepatocellular carcinoma. Aging. 2020; 13: 2803–2821.

[11] Yang X, Sun H, Song Y, Yang L, Liu H. Diagnostic and prognostic values of upregulated SPC25 in patients with hepatocellular carcinoma. PeerJ. 2020; 8: e9535.

[12] Chen F, Zhang K, Huang Y, Luo F, Hu K, Cai Q. SPC25 may promote proliferation and metastasis of hepatocellular carcinoma via p53. FEBS Open Bio. 2020; 10: 1261–1275.

[13] Shi WK, Shang QL, Zhao YF. SPC25 promotes hepatocellular carcinoma metastasis via activating the FAK/PI3K/AKT signaling pathway through ITGB4. Oncology Reports. 2022; 47: 91.

[14] Chen J, Chen H, Yang H, Dai H. SPC25 upregulation increases cancer stem cell properties in non-small cell lung ade-

nocarcinoma cells and independently predicts poor survival. Biomedicine & Pharmacotherapy. 2018; 100: 233–239.
[15] Fukuizumi A, Noro R, Seike M, Miyanaga A, Minegishi Y, Omori M, *et al*. CADM1 and SPC25 Gene Mutations in Lung Cancer Patients With Idiopathic Pulmonary Fibrosis. JTO Clinical and Research Reports. 2021; 2: 100232.
[16] Jeong J, Keum S, Kim D, You E, Ko P, Lee J, *et al*. Spindle pole body component 25 homolog expressed by ECM stiffening is required for lung cancer cell proliferation. Biochemical and Biophysical Research Communications. 2018; 500: 937–943.
[17] Cui F, Hu J, Fan Y, Tan J, Tang H. Knockdown of spindle pole body component 25 homolog inhibits cell proliferation and cycle progression in prostate cancer. Oncology Letters. 2018; 15: 5712–5720.
[18] Cui F, Tang H, Tan J, Hu J. Spindle pole body component 25 regulates stemness of prostate cancer cells. Aging. 2018; 10: 3273–3282.
[19] Wang Q, Zhu Y, Li Z, Bu Q, Sun T, Wang H, *et al*. Up-regulation of SPC25 promotes breast cancer. Aging. 2019; 11: 5689–5704.
[20] Cui F, Xu Z, Lv Y, Hu J. Role of spindle pole body component 25 in neurodegeneration. Annals of Translational Medicine. 2021; 9: 1432.
[21] Sun SC, Lee SE, Xu YN, Kim NH. Perturbation of SPC25 expression affects meiotic spindle organization, chromosome alignment and spindle assembly checkpoint in mouse oocytes. Cell Cycle (Georgetown, Tex.). 2010; 9: 4552–4559.
[22] Makker V, Green AK, Wenham RM, Mutch D, Davidson B, Miller DS. New therapies for advanced, recurrent, and metastatic endometrial cancers. Gynecologic Oncology Research and Practice. 2017; 4: 19.
[23] Zhang Y, Chen F, Chandrashekar DS, Varambally S, Creighton CJ. Proteogenomic characterization of 2002 human cancers reveals pan-cancer molecular subtypes and associated pathways. Nature Communications. 2022; 13: 2669.
[24] Chen F, Chandrashekar DS, Varambally S, Creighton CJ. Pan-cancer molecular subtypes revealed by mass-spectrometry-based proteomic characterization of more than 500 human cancers. Nature Communications. 2019; 10: 5679.
[25] Chandrashekar DS, Karthikeyan SK, Korla PK, Patel H, Shovon AR, Athar M, *et al*. UALCAN: An update to the integrated cancer data analysis platform. Neoplasia (New York, N.Y.). 2022; 25: 18–27.
[26] Uhlén M, Fagerberg L, Hallström BM, Lindskog C, Oksvold P, Mardinoglu A, *et al*. Proteomics. Tissue-based map of the human proteome. Science (New York, N.Y.). 2015; 347: 1260419.
[27] Uhlen M, Zhang C, Lee S, Sjöstedt E, Fagerberg L, Bidkhori G, *et al*. A pathology atlas of the human cancer transcriptome. Science (New York, N.Y.). 2017; 357: eaan2507.
[28] Ru B, Wong CN, Tong Y, Zhong JY, Zhong SSW, Wu WC, *et al*. TISIDB: an integrated repository portal for tumor-immune system interactions. Bioinformatics (Oxford, England). 2019; 35: 4200–4202.
[29] Vivian J, Rao AA, Nothaft FA, Ketchum C, Armstrong J, Novak A, *et al*. Toil enables reproducible, open source, big biomedical data analyses. Nature Biotechnology. 2017; 35: 314–316.
[30] Lánczky A, Győrffy B. Web-Based Survival Analysis Tool Tailored for Medical Research (KMplot): Development and Implementation. Journal of Medical Internet Research. 2021; 23: e27633.
[31] Liu J, Lichtenberg T, Hoadley KA, Poisson LM, Lazar AJ, Cherniack AD, *et al*. An Integrated TCGA Pan-Cancer Clinical Data Resource to Drive High-Quality Survival Outcome Analytics. Cell. 2018; 173: 400–416.e11.
[32] Vasaikar SV, Straub P, Wang J, Zhang B. LinkedOmics: analyzing multi-omics data within and across 32 cancer types. Nucleic Acids Research. 2018; 46: D956–D963.
[33] Szklarczyk D, Gable AL, Nastou KC, Lyon D, Kirsch R, Pyysalo S, *et al*. The STRING database in 2021: customizable protein-protein networks, and functional characterization of user-uploaded gene/measurement sets. Nucleic Acids Research. 2021; 49: D605–D612.
[34] Belinky F, Nativ N, Stelzer G, Zimmerman S, Iny Stein T, Safran M, *et al*. PathCards: multi-source consolidation of human biological pathways. Database: the Journal of Biological Databases and Curation. 2015; 2015: bav006.
[35] Klutstein M, Nejman D, Greenfield R, Cedar H. DNA Methylation in Cancer and Aging. Cancer Research. 2016; 76: 3446–3450.
[36] Győrffy B, Bottai G, Fleischer T, Munkácsy G, Budczies J, Paladini L, *et al*. Aberrant DNA methylation impacts gene expression and prognosis in breast cancer subtypes. International Journal of Cancer. 2016; 138: 87–97.
[37] Modhukur V, Iljasenko T, Metsalu T, Lokk K, Laisk-Podar T, Vilo J. MethSurv: a web tool to perform multivariable survival analysis using DNA methylation data. Epigenomics. 2018; 10: 277–288.
[38] Bharadwaj R, Qi W, Yu H. Identification of two novel components of the human NDC80 kinetochore complex. The Journal of Biological Chemistry. 2004; 279: 13076–13085.
[39] Baylin SB, Jones PA. A decade of exploring the cancer epigenome - biological and translational implications. Nature Reviews. Cancer. 2011; 11: 726–734.
[40] Irizarry RA, Ladd-Acosta C, Wen B, Wu Z, Montano C, Onyango P, *et al*. The human colon cancer methylome shows similar hypo- and hypermethylation at conserved tissue-specific CpG island shores. Nature Genetics. 2009; 41: 178–186.
[41] Slack FJ, Chinnaiyan AM. The Role of Non-coding RNAs in Oncology. Cell. 2019; 179: 1033–1055.
[42] Li S, Liu M, Do MH, Chou C, Stamatiades EG, Nixon BG, *et al*. Cancer immunotherapy via targeted TGF-β signalling blockade in T_H cells. Nature. 2020; 587: 121–125.
[43] Quail DF, Joyce JA. Microenvironmental regulation of tumor progression and metastasis. Nature Medicine. 2013; 19: 1423–1437.
[44] Hong S, Qian J, Yang J, Li H, Kwak LW, Yi Q. Roles of idiotype-specific t cells in myeloma cell growth and survival: Th1 and CTL cells are tumoricidal while Th2 cells promote tumor growth. Cancer Research. 2008; 68: 8456–8464.
[45] Jin YW, Hu P. Tumor-Infiltrating CD8 T Cells Predict Clinical Breast Cancer Outcomes in Young Women. Cancers. 2020; 12: 1076.
[46] Pauken KE, Wherry EJ. Overcoming T cell exhaustion in infection and cancer. Trends in Immunology. 2015; 36: 265–276.
[47] Crinier A, Narni-Mancinelli E, Ugolini S, Vivier E. SnapShot: Natural Killer Cells. Cell. 2020; 180: 1280–1280.e1.
[48] Eruslanov EB, Bhojnagarwala PS, Quatromoni JG, Stephen TL, Ranganathan A, Deshpande C, *et al*. Tumor-associated neutrophils stimulate T cell responses in early-stage human lung cancer. The Journal of Clinical Investigation. 2014; 124: 5466–5480.
[49] Fu C, Jiang A. Dendritic Cells and CD8 T Cell Immunity in Tumor Microenvironment. Frontiers in Immunology. 2018; 9: 3059.
[50] Snyder A, Makarov V, Merghoub T, Yuan J, Zaretsky JM, Desrichard A, *et al*. Genetic basis for clinical response to CTLA-4 blockade in melanoma. The New England Journal of Medicine. 2014; 371: 2189–2199.
[51] Tumeh PC, Harview CL, Yearley JH, Shintaku IP, Taylor EJM, Robert L, *et al*. PD-1 blockade induces responses by inhibiting adaptive immune resistance. Nature. 2014; 515: 568–571.
[52] Ley K. Arrest chemokines. Microcirculation (New York, N.Y.: 1994). 2003; 10: 289–295.

[53] Kanemitsu N, Ebisuno Y, Tanaka T, Otani K, Hayasaka H, Kaisho T, *et al*. CXCL13 is an arrest chemokine for B cells in high endothelial venules. Blood. 2005; 106: 2613–2618.
[54] Pallandre JR, Krzewski K, Bedel R, Ryffel B, Caignard A, Rohrlich PS, *et al*. Dendritic cell and natural killer cell cross-talk: a pivotal role of CX3CL1 in NK cytoskeleton organization and activation. Blood. 2008; 112: 4420–4424.
[55] Lee SS, Cheah YK. The Interplay between MicroRNAs and Cellular Components of Tumour Microenvironment (TME) on Non-Small-Cell Lung Cancer (NSCLC) Progression. Journal of Immunology Research. 2019; 2019: 3046379.
[56] Azimi F, Scolyer RA, Rumcheva P, Moncrieff M, Murali R, McCarthy SW, *et al*. Tumor-infiltrating lymphocyte grade is an independent predictor of sentinel lymph node status and survival in patients with cutaneous melanoma. Journal of Clinical Oncology: Official Journal of the American Society of Clinical Oncology. 2012; 30: 2678–2683.
[57] Peng D, Kryczek I, Nagarsheth N, Zhao L, Wei S, Wang W, *et al*. Epigenetic silencing of TH1-type chemokines shapes tumour immunity and immunotherapy. Nature. 2015; 527: 249–253.
[58] Nagarsheth N, Wicha MS, Zou W. Chemokines in the cancer microenvironment and their relevance in cancer immunotherapy. Nature Reviews. Immunology. 2017; 17: 559–572.
[59] Zlotnik A, Yoshie O. The chemokine superfamily revisited. Immunity. 2012; 36: 705–716.
[60] Matsukawa A, Hogaboam CM, Lukacs NW, Lincoln PM, Evanoff HL, Kunkel SL. Pivotal role of the CC chemokine, macrophage-derived chemokine, in the innate immune response. Journal of Immunology (Baltimore, Md.: 1950). 2000; 164: 5362–5368.
[61] Ness TL, Ewing JL, Hogaboam CM, Kunkel SL. CCR4 is a key modulator of innate immune responses. Journal of Immunology (Baltimore, Md.: 1950). 2006; 177: 7531–7539.
[62] Hogg SJ, Beavis PA, Dawson MA, Johnstone RW. Targeting the epigenetic regulation of antitumour immunity. Nature Reviews. Drug Discovery. 2020; 19: 776–800.